Differentiation of Monkey Embryonic Stem Cells to Hepatocytes by Feeder-Free Dispersion Culture and Expression Analyses of Cytochrome P450 Enzymes Responsible for Drug Metabolism

Junya Maruyama,[a] Tamihide Matsunaga,[b] Satoshi Yamaori,[a] Sakae Sakamoto,[c] Noboru Kamada,[c] Katsunori Nakamura,[b] Shinji Kikuchi,[c] and Shigeru Ohmori*[,a]

[a] *Department of Pharmacy, Shinshu University Hospital; 3–1–1 Asahi, Matsumoto 390–8621, Japan:* [b] *Graduate School of Pharmaceutical Sciences, Nagoya City University; 3–1 Tanabe-dori, Mizuho-ku, Nagoya 467–8603, Japan: and* [c] *Kissei Pharmaceutical Co., Ltd.; 4365–1 Kashiwabara, Hotaka, Azumino 399-8304, Japan.*
Received October 3, 2012; accepted November 15, 2012; advance publication released online December 8, 2012

We reported previously that monkey embryonic stem cells (ESCs) were differentiated into hepatocytes by formation of embryoid bodies (EBs). However, this EB formation method is not always efficient for assays using a large number of samples simultaneously. A dispersion culture system, one of the differentiation methods without EB formation, is able to more efficiently provide a large number of feeder-free undifferentiated cells. A previous study demonstrated the effectiveness of the Rho-associated kinase inhibitor Y-27632 for feeder-free dispersion culture and induction of differentiation of monkey ESCs into neural cells. In the present study, the induction of differentiation of cynomolgus monkey ESCs (cmESCs) into hepatocytes was performed by the dispersion culture method, and the expression and drug inducibility of cytochrome P450 (CYP) enzymes in these hepatocytes were examined. The cmESCs were successfully differentiated into hepatocytes under feeder-free dispersion culture conditions supplemented with Y-27632. The hepatocytes differentiated from cmESCs expressed the mRNAs for three hepatocyte marker genes (α-fetoprotein, albumin, CYP7A1) and several CYP enzymes, as measured by real-time polymerase chain reaction. In particular, the basal expression of cmCYP3A4 (3A8) in these hepatocytes was detected at mRNA and enzyme activity (testosterone 6β-hydroxylation) levels. Furthermore, the expression and activity of cmCYP3A4 (3A8) were significantly upregulated by rifampicin. These results indicated the effectiveness of Y-27632 supplementation for feeder-free dispersed culture and induction of differentiation into hepatocytes, and the expression of functional CYP enzyme(s) in cmESC-derived hepatic cells.

Key words embryonic stem cell; differentiation; hepatocyte; monkey; cytochrome P450; feeder-free dispersed culture

Investigation of drug metabolism with human hepatocytes is important in the early stages of drug development. However, primary human hepatocytes are short-lived and cannot be maintained in culture over the long term. In addition, there are large donor-dependent variations in drug metabolism. On the other hand, human embryonic stem cells (ESCs) are able to replicate infinitely and differentiate into various types of somatic cells including germ cells.[1] Thus, they represent an attractive source to provide large numbers of cells that can be utilized for the development of candidate drug-screening strategies in place of primary cells.[2] However, ethical and legal restrictions have limited the availability of human ESCs. The phenotype of human ESCs is known to closely resemble that of monkey ESCs but not mouse ESCs with regard to morphology, leukemia inhibitory factor responsiveness, gene expression profiles, and some disease models.[1,3–6] Thus, monkey ESCs are a more suitable model for preclinical research of drug development. In particular, hepatocytes derived from monkey ESCs may be useful for pharmacokinetic studies, such as investigation of drug–drug interactions and the inducibility of drug-metabolizing enzymes, including cytochrome P450 (CYP).

We reported previously that monkey ESCs were successfully differentiated into hepatocytes by the formation of embryoid bodies (EBs) and treatment with specific growth factors and cytokines critical for hepatic differentiation.[7] EBs can mimic the inductive microenvironment required for liver organogenesis[8–10] and develop into many different cell types in culture. However, this EB formation method is not always appropriate for assays with large numbers of samples, such as high-throughput screening, because the formation of EBs is inefficient. A dispersion culture system, one of the differentiation methods without EB formation, can more efficiently provide a large number of feeder-free undifferentiated cells. The Rho-associated kinase (ROCK) inhibitor Y-27632 enables expansion from single-cell culture of human ESCs under dispersion culture conditions because the ROCK inhibitor markedly reduces dissociation-induced apoptosis of human ESCs.[11] Furthermore, Takehara *et al.*[12] conducted direct neural stem cell induction from cynomolgus monkey (*Macaca fascicularis*) ESCs (cmESCs) using Y-27632 and demonstrated the effectiveness of Y-27632 supplementation for feeder-free culture and induction of differentiation. However, it is not clear whether this dispersion culture method is effective for differentiation of monkey ESCs into hepatocytes.

In the present study, we carried out induction of hepatocyte differentiation from cmESCs by the dispersion culture method and examined expression and drug inducibility of CYP in the differentiated cells.

MATERIALS AND METHODS

Materials Growth Factor Reduced BD Matrigel Matrix (Matrigel reduced) was obtained from BD Biosciences

The authors declare no conflict of interest.

*To whom correspondence should be addressed. e-mail: somori@shinshu-u.ac.jp

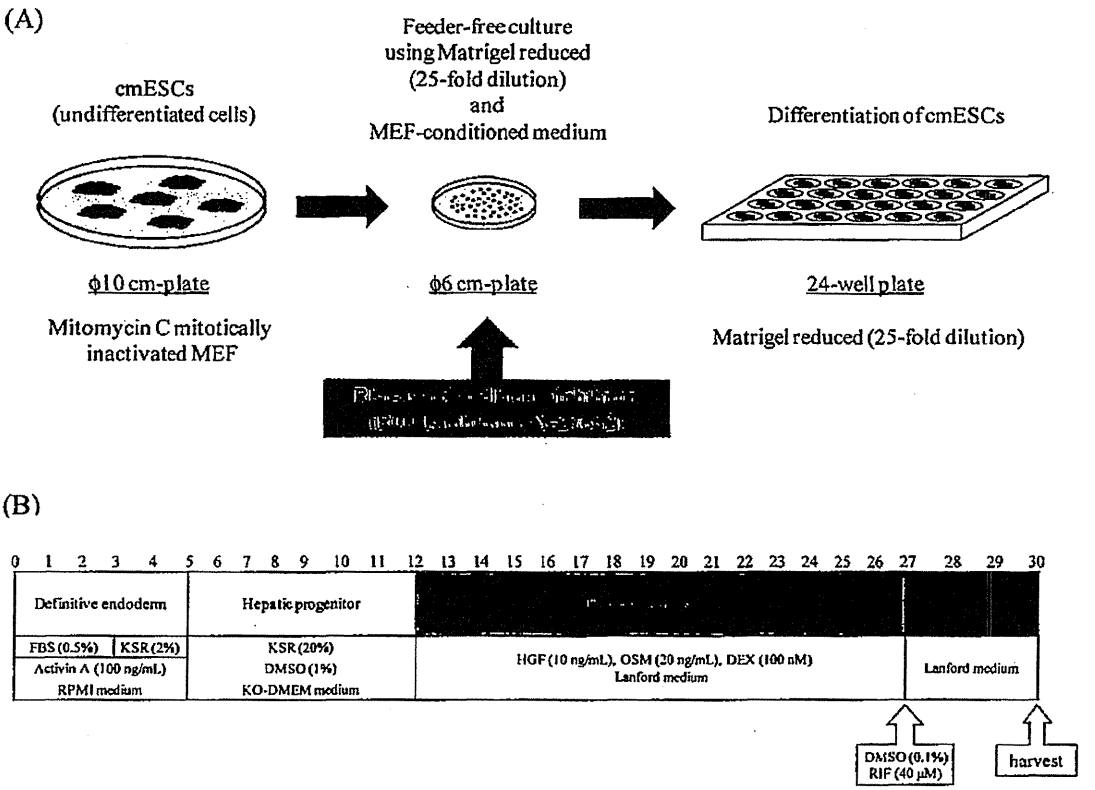

Fig. 1. Scheme of *in Vitro* Differentiation of cmESCs into Hepatocytes

(A) Illustration of the feeder-free dispersion culture of undifferentiated cmESCs. (B) Schematic procedure of differentiation of cmESCs into hepatocytes and drug treatment.

(Bedford, MA, U.S.A.); mitomycin C, Dulbecco's modified Eagle's medium (DMEM), William's E medium with GlutaMAX without phenol red, MEM non-essential amino acid solution (100×), and 6β-hydroxytestosterone from Sigma (St. Louis, MO, U.S.A.); murine embryonic fibroblasts (MEF) from Oriental Yeast (Tokyo, Japan); RPMI1640 medium supplemented with GlutaMAX, KnockOut™ DMEM, KnockOut Serum Replacement (KSR), minimum essential medium (MEM), L-glutamine, 0.25% (w/v) trypsin-ethylenediaminetetraacetic acid (EDTA), and SuperScript™ III First-Strand Synthesis System for reverse transcription-polymerase chain reaction (RT-PCR) from Invitrogen Life Technologies (Carlsbad, CA, U.S.A.); fetal bovine serum (FBS) from Equitech-Bio, Inc. (Kerrville, TX, U.S.A.); recombinant human activin A and recombinant human hepatocyte growth factor (HGF) from Funakoshi Co., Ltd. (Tokyo, Japan); modified Lanford medium from Charles River Laboratories Japan Inc. (Yokohama, Japan); recombinant human basic fibroblast growth factor (bFGF), Y-27632, oncostatin M (OSM), dexamethasone (DEX), rifampicin (RIF), testosterone, and dimethyl sulfoxide (DMSO) from Wako Pure Chemicals (Osaka, Japan); [$^2H_7$]6β-hydroxytestosterone from BD Gentest (Franklin Lakes, NJ, U.S.A.); illustra RNAspin Mini RNA Isolation kit from GE Healthcare (Tokyo, Japan); SYBR® Green real-time PCR Master Mix from TaKaRa Bio (Otsu, Japan). All other reagents used were of the highest quality available.

ESC Culture and Differentiation The cmESCs (CMK6) were generously provided by Tanabe Seiyaku Co., Ltd. (Osaka, Japan)[4] and maintained according to the method reported previously[7] except that recombinant human bFGF was added to ES medium. Feeder-free dispersed culture was carried out as follows (Fig. 1A). The cmESCs were cultured in the presence of 10 μM Y-27632 for 1 h before detaching the cells from the feeder layer. After detachment of the cmESCs, contaminating MEF were removed by incubating the cell suspension on gelatin-coated plates (BD Falcon, Franklin Lakes, NJ, U.S.A.) at 37°C for 2 h. The cmESC clumps were recovered from the suspension by centrifugation, incubated in 0.25% (w/v) trypsin-EDTA solution at 37°C for 5 min, and dissociated into single cells by pipetting. The cells were passed through a Cell Strainer (40 μm mesh; BD Falcon) and seeded onto culture plates 6 cm in diameter (BD Falcon) coated with Matrigel reduced (25-fold dilution). The cmESCs were cultured in medium conditioned by contact with MEF with 4 ng/mL recombinant human bFGF and 10 μM Y-27632 for the first 24 h. The medium was changed for MEF-conditioned medium for cmESCs without Y-27632.

When cmESCs reached approximately 70% confluence, differentiation was initiated by replacing RPMI1640 medium supplemented with GlutaMax containing 0.5% FBS and 100 ng/mL activin A (Fig. 1B). After 72 h, the medium was changed to RPMI1640 medium supplemented with GlutaMax containing 2% KSR and 100 ng/mL activin A, and culture was continued for 48 h. The cells were passaged onto 24-well plates coated with Matrigel reduced (25-fold dilution) and cultured in KnockOut™ DMEM containing 20% KSR, 1 mM L-glutamine, 1% MEM nonessential amino acids, and 1% DMSO for 7 d. Finally, the cells were cultured in modified Lanford medium containing 10 ng/mL HGF, 20 ng/mL OSM, and 100 nM DEX. The medium was changed daily during differentiation.

Table 1. Primers Used for Real-Time PCR Analysis

Genes	Forward primer (5'–3')	Reverse primer (5'–3')	Product (bp)
AFP	ACTATTGGCCTGTGGTGAGG	CACCCTGAGCTTGACACAGA	224
ALB	CTTCCTGGGCATGTTTTTGT	GGCTCTTCCACAAGAGGTTG	177
CYP1A1	CTAGACACAGTGATTGGCAGGTC	GGTTGACCCATAGCTTCTGGTCA	232
cmCYP2B6 (2B30)	GGGGCATTGAAGAAGAATGA	ATTTTGCCCACACCACTCTC	188
cmCYP2C9 (2C43)	TGATTCCCAAGGGTACAACC	AAATTGCCACCTTCATCCAG	118
cmCYP2D6 (2D17)	AGATCGACGACGTGATAGGG	GTCCCCTTAGGGATGAGGAA	178
cmCYP3A4 (3A8)	CCAAGAAGCTTTTAAGATTTGATTTC	ATCTACTCGGTGCTTTTGTGTA	191
cmCYP3A5 (3A66)	TTTGCCCAATAAGGCACCTG	GGTTGGAATCACCACCATTG	181
CYP7A1	ATTTGGTGCCAATCCTCTTG	CATCCTTTGGGTCAATGCTT	215
AhR	ACTCCACTTCAGCCACCATC	CTCGTGCACAGTTCTGCTTC	146
PXR	AAGGATGCAAGGGCTTTTTC	TTCTTCATGCCGCTCTCC	151
GAPDH	GTCAGTGGACCTGACCT	TGCTGTAGCCAAATTCGTTG	245

AFP, α-fetoprotein; ALB, albumin; AhR, aryl hydrocarbon receptor; PXR, pregnane X receptor; GADPH, glyceraldehyde-3-phosphate dehydrogenase.

Drug Treatment To clarify the effects of RIF on expression of CYP, cmESC-derived hepatocytes were treated with 40 μM RIF for 72 h (Fig. 1B). The compound was dissolved in DMSO, which was added to the modified Lanford medium at a final concentration of 0.1%.

Primary Hepatocyte Culture Primary cynomolgus monkey hepatocytes (primary cmHCs, Batch HEP 18605) were obtained from BIOPREDIC International (Renes, France). The primary cmHCs were thawed according to the manufacturer's instructions. Briefly, the primary cmHCs were cultured on 24-well plates (BD Falcon) in William's E medium with GlutaMax without phenol red for 72 h, and the medium was changed daily.

Real-time PCR Analysis Total RNA was isolated from the cells and the liver of an adult male monkey (Ina Research Inc., Ina, Japan) using the illustra RNAspin Mini RNA Isolation kit according to the manufacturer's protocol. First-strand cDNA was generated from 5 μg of total RNA. Reverse transcription reaction was performed using the SuperScript™ III First-Strand Synthesis System for RT-PCR in accordance with the manufacturer's instructions. For detection of mRNA expression levels, CYP mRNAs were analyzed by SYBR® Green real-time quantitative PCR. All PCR procedures were performed using the ABI Prism 7300 Real-time PCR System (Applied Biosystems, Foster City, CA, U.S.A.). PCR was performed in a mixture consisting of 10 μL of SYBR® Green real-time PCR Master Mix, 0.4 μL of 10 μM forward and reverse primers, 0.4 μL of dye, 7.8 μL of water, and 1 μL template cDNA in a total of 20 μL. The primers used are summarized in Table 1. The levels of these mRNAs were normalized relative to that of glyceraldehyde-3-phosphate dehydrogenase (GAPDH) mRNA.

Measurement of Cellular Activity of Testosterone 6β-Hydroxylation Following drug treatment, cmESC-derived hepatocytes were incubated with 100 μM testosterone in modified Lanford medium for 6 h. On the other hand, primary cmHCs were incubated with 100 μM testosterone in MEM for 6 h. After incubation, each medium was collected and 6β-hydroxytestosterone was measured by LC-MS/MS under the conditions described below.

Instrument An Agilent 1100 series HPLC system (Agilent Technologies, Waldbronn, Germany) consisting of a binary pump, a degasser linked to a CTC HTS PAL New Wash System Autosampler (AMR Inc., Tokyo, Japan) was used.

Table 2. Timetable for HPLC

Time (min)	Solvent A (%)	Solvent B (%)
0	10	90
3	10	90
6	90	10
9	90	10
9.1	10	90
16	10	90

Solvents A: 10 mM ammonium acetate in water. Solvents B: 0.1% formic acid in methanol.

Mass spectrometry was performed on an API 4000 triple quadruple instrument (Applied Biosystems/Sciex, Foster City, CA, U.S.A.) equipped with a TurboIonSpray® electrospray ionization (ESI) interface. Data processing was performed with the Analyst 1.4.2 software package (Applied Biosystems/Sciex).

Chromatographic Conditions Chromatographic separation was performed on a reversed-phase CAPCELL PAK C18 MG III column (50×4.6 mm i.d., 5 μm; Shiseido Co., Inc., Tokyo, Japan). The column temperature was kept constant at 40°C. The mobile phase consisted of a mixture of 10 mM ammonium acetate in water (A) with 0.1% formic acid in methanol (B) and was delivered at a flow rate of 0.5 mL/min. A stepwise gradient was used as shown in Table 2.

Mass Spectrometry Conditions The mass spectrometer was operated using the ESI source in positive ion mode. To optimize all of the MS parameters, standard solutions (100 ng/mL) and internal standard were infused into the mass spectrometer at a flow rate of 250 μL/min. The ion spray voltage (IS) was set at 4500 V. The TurboIonSpray probe temperature was maintained at 600°C. The instrument parameters *viz.*, nebulizer gas, curtain gas, auxiliary gas, and collision gas, were set at 60, 15, 80, and 5, respectively. Compound parameters *viz.*, declustering potential, collision energy, entrance potential, and collision exit potential, were 40, 20, 10, and 15, respectively, for 6β-hydroxytestosterone and [$^2H_7$]6β-hydroxytestosterone. Zero air was used as the source gas, while nitrogen was used as both curtain and collision gas. The mass spectrometer was operated in ESI positive ion mode and detection of the ions was performed in the multiple reaction monitoring (MRM) mode, monitoring the transition of *m/z* 305 precursor ion [M+H] to the *m/z* 269 product ion for 6β-hydroxytestosterone (retention time 8.7 min) and *m/z* 312 precursor ion [M+H] to the *m/z* 276 product ion for

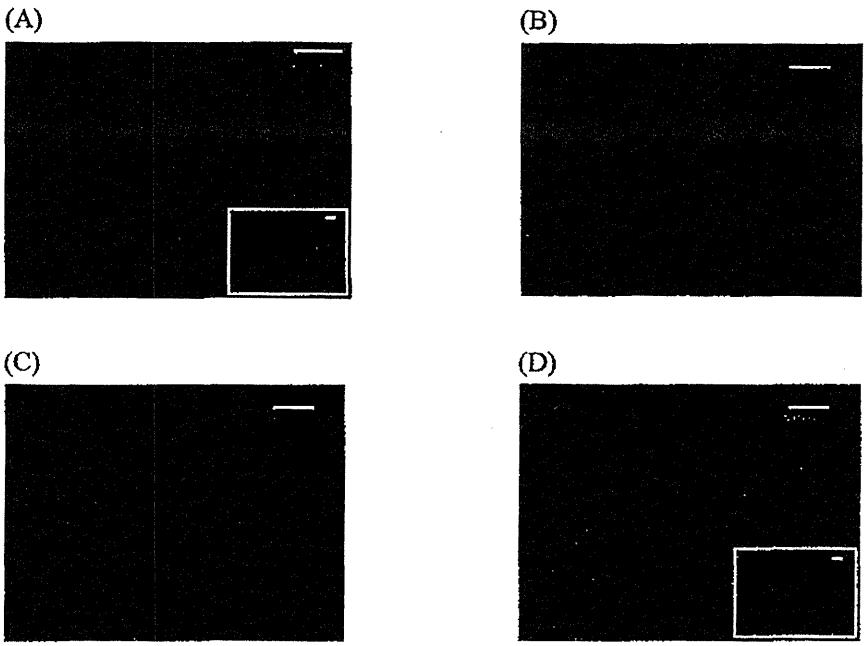

Fig. 2. Morphology of cmESCs in Individual Culture Processes

(A) Undifferentiated cmESCs. (B) Suspended cmESCs incubated on gelatin-coated plates for 2 h. (C) cmESCs cultured on plates 6 cm in diameter coated with Matrigel reduced (25-fold dilution) for 24 h. (D) cmESC-derived cells at 27 d after the initiation of hepatocyte differentiation. The cells were visualized by phase microscopy. Bars, 200 μm; 30 μm for A and D insets.

[$^2H_7$]6β-hydroxytestosterone (8.7 min). Quadrupoles Q1 and Q3 were set to unit resolution. Data acquisition and quantification were performed using Analyst software version 1.4.2 (Applied Biosystems, MDS Sciex, Toronto, ON, Canada).

Calibration Standards Calibration standards to cover the assay range of 10–5000 nM 6β-hydroxytestosterone were prepared by adding 10 μL of 0.1, 0.5, 1, 5, 10, and 50 μM working standards to 0.1 mL aliquots of control reaction mixture.

Statistical Analysis Statistical significance was assessed using the unpaired t test. In all analyses, $p < 0.05$ was taken to indicate statistical significance.

RESULTS

Morphology of cmESCs at Individual Culture Steps A typical colony of undifferentiated cmESCs is shown in Fig. 2A. As reported previously for primate ESCs, undifferentiated cmESCs formed tightly packed and flat colonies.[4] Each cell had a high nucleus/cytoplasm ratio and prominent nucleolus. In an effort to circumvent the problem of apoptosis in cmESC culture, the single-cell dispersed culture was performed under feeder-free cell culture conditions using Y-27632. The undifferentiated cmESCs were cultured in the presence of 10 μM Y-27632 for 1 h before detaching the cells from the feeder layer. After the cmESC colonies were dissociated by trypsin and suspended, the cells were seeded on gelatin-coated plates. In this procedure, contaminating MEF adhered to the plate bottom, whereas the cmESCs did not (Fig. 2B). The cmESC clumps were recovered from the suspension and dissociated into single cells by pipetting. The single cells were cultured on culture plates 6 cm in diameter coated with Matrigel reduced (25-fold dilution) in the presence of 10 μM Y-27632 for first 24 h. The cmESCs proliferated on the feeder-free culture plates (Fig. 2C). Twenty-seven days after initiation of hepatocyte differentiation, cells showed characteristic morphologies of hepatocytes, *i.e.*, polygonal in shape and multiple nuclei (Fig. 2D). Y-27632 was effective for cmESC survival under dispersion culture conditions.

Expression of Hepatocyte Markers and CYP Enzymes in Primary cmHCs and cmESC-Derived Hepatocytes The mRNA expression levels of hepatocyte marker genes and CYP enzymes in primary cmHCs and differentiated cells from cmESCs were measured by a real-time PCR method. As shown in Fig. 3, the mRNAs of hepatocyte marker genes, α-fetoprotein (AFP), albumin (ALB), and CYP7A1, were detected in cmESC-derived hepatocytes together with those of CYP1A1, cmCYP2B6 (2B30), cmCYP2C9 (2C43), cmCYP2D6 (2D17), cmCYP3A4 (3A8), cmCYP3A5 (3A66), pregnane X receptor (PXR), and aryl hydrocarbon receptor (AhR). The mRNA levels of AFP and CYP7A1 in differentiated cells from cmESCs were 16- and 21-fold, respectively, higher than those in primary cmHCs, although the expression level of ALB was approximately 80-fold lower in cmESC-derived hepatocytes than in primary cmHCs. The mRNA levels of CYP1A1, cmCYP2B6 (2B30), cmCYP2C9 (2C43), cmCYP2D6 (2D17), cmCYP3A4 (3A8), cmCYP3A5 (3A66), and PXR in the cells differentiated from cmESCs were 386-, 7.4-, 284-, 1.6-, 136-, 5.9-, and 13-fold, respectively, lower than those in primary cmHCs. In contrast, the expression level of AhR mRNA in cmESC-derived hepatocytes was 2.2-fold higher than that in primary cmHCs.

Testosterone 6β-Hydroxylase Activity of Primary cmHCs and cmESC-Derived Hepatocytes Testosterone 6β-hydroxylase activity as a marker of CYP3A, especially cmCYP3A4 (3A8), was evaluated with primary cmHCs and cmESC-derived hepatocytes. Testosterone 6β-hydroxylase activity was detected in the cells differentiated from cmESCs (Fig. 4). The activity was about one sixth that of the primary

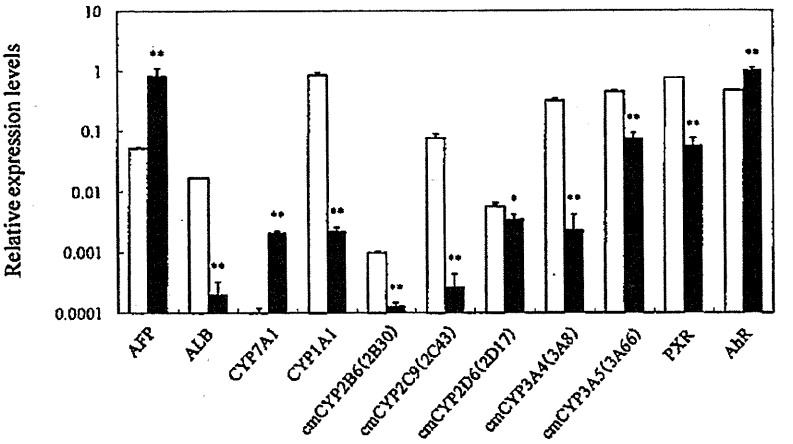

Fig. 3. Expression Levels of mRNAs for Hepatocyte Markers and CYP Enzymes in Primary cmHCs and cmESC-Derived Hepatocytes

Target mRNAs were analyzed by SYBR Green real-time PCR as described in Materials and Methods. Data are presented as the relative levels (means±S.D., n=3) of primary cmHCs (open columns) or cmESC-derived hepatocytes (closed columns) to adult monkey liver. Significantly different from primary cmHCs ($^{*}p < 0.05$, $^{**}p < 0.01$).

cmHCs.

Effects of RIF on the Expression Level and Activity of cmCYP3A4 (3A8) in the Cells Differentiated from cmESCs The induction potency of cmCYP3A4 (3A8) by RIF, which is known as a cmCYP3A4 (3A8) inducer,[13,14] was examined with the cells differentiated from cmESCs. The expression of cmCYP3A4 (3A8) mRNA was significantly induced by RIF in the cmESC-derived hepatocytes (Fig. 5A). The activity of testosterone 6β-hydroxylase in the cmESC-derived hepatocytes was significantly enhanced by RIF (Fig. 5B).

DISCUSSION

The method to induce differentiation of ESCs to hepatic cells was first established using mouse cells.[15–17] Many of these methods involve a procedure to differentiate ESCs by EB formation and adhesion culture. EBs differentiate into three embryonic germ layers by suspended cell culture of ESCs, and these cells can then further differentiate into multiple cell types, including hepatocytes, *in vitro*.[18] This method was applied to the induction of differentiation of monkey ESCs into hepatic cells.[7] In recent studies, however, a method to add some direct inducing factors to a monolayer culture system of an undifferentiated ESC colony without EB formation has been used extensively. Furthermore, some improved methods for more efficient differentiation into hepatocytes have been reported. Among these methods, the stepwise addition of two or more factors is most common.[19–23] However, if these complicated operations are not performed adequately, the death of ESCs can easily occur. In previous culture systems, remarkable reduction of the number of live cells was a technical obstacle to the induction of differentiation. Watanabe *et al.*[11] found that the death of human ESCs occurring after cell dissociation is triggered by activation of ROCK, and that the ROCK inhibitor Y-27632 can control the death of ESCs. Interestingly, Takehara *et al.*[12] demonstrated that Y-27632 also promotes survival of cmESCs and enables expansion from single cells without loss of their pluripotent characteristics. These findings suggest that reactions to the ROCK inhibitor may be preserved in primate ESCs. In addition, it has been shown that Y-27632 supplementation also enables cmESC

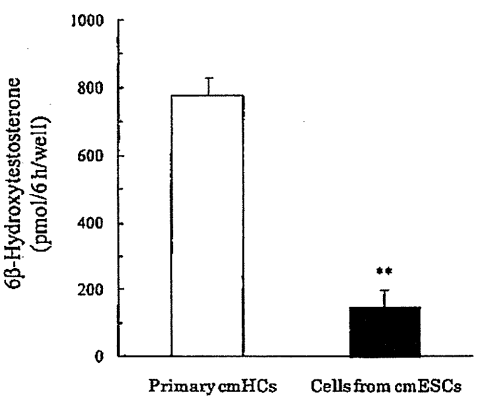

Fig. 4. Testosterone 6β-Hydroxylase Activity of Primary cmHCs and cmESC-Derived Hepatocytes

Primary cmHCs and cmESC-derived hepatocytes were incubated with testosterone at a final concentration of 100μM for 6h. Testosterone 6β-hydroxylase activity as a marker of CYP3A, especially cmCYP3A4 (3A8), was measured by LC-MS/MS as described in Materials and Methods. Values are expressed as the means±S.D. (n=3). Significantly different from primary cmHCs ($^{**}p<0.01$).

expansion in feeder-free culture.[12] Feeder cells supply secretory components, extracellular matrix, and intercellular contacts for maintenance of an undifferentiated state and pluripotency of ESCs. However, the use of feeder cells leads to the potential for cross-contamination, such as the passing of animal pathogens to ESCs. On the other hand, feeder-free culture is a system to maintain ESCs in an undifferentiated state without direct contact with feeder cells. The ROCK inhibitor, Y-27632, is an important factor to enable adhesion and proliferation of primate ESCs in feeder-free culture. In the present study, we confirmed that dissociated cmESCs treated with Y-27632 were protected from cell death in feeder-free culture and formed clumps (Fig. 2B). Furthermore, the cells differentiated from cmESCs showed multinuclear morphology characteristic of hepatocytes at the final stage of differentiation (Fig. 2D). This feeder-free dispersion culture method was reproducible without any technical obstacles.

Although ALB is the most abundant protein synthesized by mature hepatocytes, its expression starts in early fetal hepatocytes and reaches the maximal level in adult hepatocytes.[24] Our study showed that the expression of ALB mRNA in

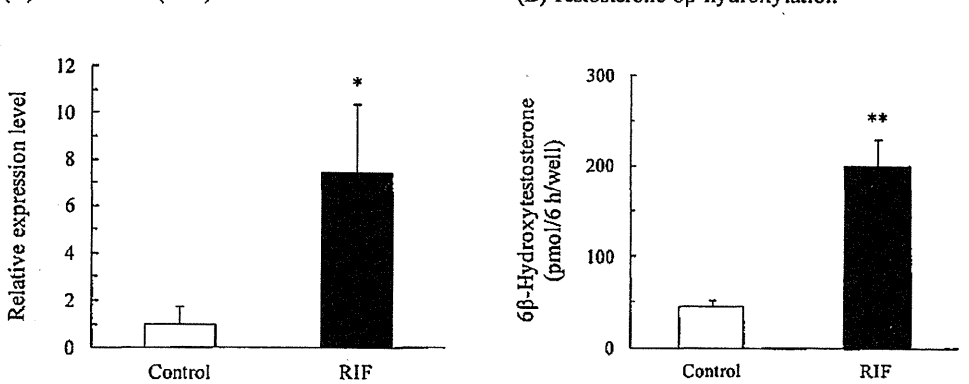

Fig. 5. Effects of RIF on cmCYP3A4 (3A8) mRNA Expression Level and Testosterone 6β-Hydroxylase Activity in Cells Differentiated from cmESCs

cmESC-Derived hepatocytes were treated with vehicle (0.1% DMSO) or 40 μM RIF for 72h. After treatment with RIF, the cells were incubated with testosterone at a concentration of 100 μM for 6h. (A) cmCYP3A4 (3A8) mRNA was analyzed by SYBR Green real-time PCR as described in Materials and Methods. Data are presented as the relative levels (means±S.D., n=3) of RIF treatment to vehicle treatment. (B) Testosterone 6β-hydroxylase activity was measured by LC-MS/MS as described in Materials and Methods. Significantly different from control (*p<0.05, **p<0.01).

hepatocytes differentiated from cmESCs was markedly lower than in primary cmHCs and adult monkey liver. On the other hand, AFP is a marker of endodermal differentiation as well as an early fetal hepatic marker; its expression level decreases as the liver develops into the adult phenotype. In this study, the expression of AFP mRNA in cmESC-derived hepatocytes was higher than that in primary cmHCs, although the mRNA level in the former cells was comparable to that in adult monkey liver. These results suggest that cmESC-derived hepatocytes may be differentiated into more immature cells rather than into mature cells.

CYP1A1 is a major CYP1A isoform expressed in the monkey liver,[25] in contrast to the human liver, which mainly expresses CYP1A2 but not CYP1A1.[26] cmCYP2B6 (2B30), cmCYP2C9 (2C43), cmCYP2D6 (2D17), cmCYP3A4 (3A8), and cmCYP3A5 (3A66) are major CYP enzymes in the cynomolgus monkey liver.[27] These monkey CYP enzymes show a high degree of amino acid sequence identity (>90%) with corresponding human CYP enzymes and catalyze typical drug oxidations of corresponding human CYP isoforms.[28] To characterize the expression of CYP1A1, cmCYP2B6 (2B30), cmCYP2C9 (2C43), cmCYP2D6 (2D17), cmCYP3A4 (3A8), and cmCYP3A5 (3A66) in hepatocytes differentiated from cmESCs, the basal gene expression patterns of these CYP enzymes were compared with primary cmHCs. The expression levels of the CYP enzymes examined were lower in cmESC-derived hepatocytes than in primary cmHCs. The lower expression of these CYP enzymes may be associated with hepatocyte maturity. In this study, the cmESC-derived hepatic cells were found to express cmCYP3A4 (3A8) mRNA. This enzyme function in differentiated hepatocytes was confirmed by testosterone 6β-hydroxylase activity. To our knowledge, this is the first study showing the functional expression of certain CYP enzyme in cmESC-derived hepatic cells. Furthermore, these cells showed inducibility of cmCYP3A4 (3A8) by RIF at mRNA and activity levels. This inducibility was qualitatively reproducible. The effects of RIF on mRNA expression of cmCYP3A4 (3A8) in the cmESC-derived hepatic cells was consistent with the findings reported previously.[7] It was previously reported that cmCYP3A4 (3A8) is induced by RIF through the transcription factor PXR.[29] Our study showed that PXR is expressed in cmESC-derived hepatic cells. These results suggest that PXR is active in these hepatocytes. This has important implications for the application of cmESC-derived hepatic cells as an *in vitro* model for drug development. However, the functional significance of cmCYP3A4 (3A8) and PXR in cmESC-derived hepatocytes was limited in this study because the data were partially qualitative. Further improvements are required, particularly with regard to maturation and quantitative analysis, for use of cmESC-derived hepatocytes in drug screening.

In conclusion, cmESCs were successfully differentiated into hepatocytes under feeder-free dispersion culture conditions supplemented with Y-27632. In addition, the basal expression and drug inducibility of CYP enzymes were characterized in these hepatocytes. These results suggest that cmESC-derived hepatocytes may be used as a potential source for stable supply of hepatocytes for drug metabolism analysis, although further investigations are needed to improve this method.

Acknowledgments This work was partly supported by Grants-in-Aid from the Ministry of Education, Culture, Sports, Science and Technology of Japan (Nos. 20926015, 22926013, and 23926012). We also thank Ms. K. Aikawa for technical assistance. We are grateful to Tanabe Seiyaku Co., Ltd. (Osaka, Japan) for generously providing cmESCs (CMK6).

REFERENCES

1) Thomson JA, Itskovitz-Eldor J, Shapiro SS, Waknitz MA, Swiergiel JJ, Marshall VS, Jones JM. Embryonic stem cell lines derived from human blastocysts. *Science*, 282, 1145–1147 (1998).
2) Davila JC, Cezar GG, Thiede M, Strom S, Miki T, Trosko J. Use and application of stem cells in toxicology. *Toxicol. Sci.*, 79, 214–223 (2004).
3) Reubinoff BE, Pera MF, Fong CY, Trounson A, Bongso A. Embryonic stem cell lines from human blastocysts: somatic differentiation *in vitro*. *Nat. Biotechnol.*, 18, 399–404 (2000).
4) Suemori H, Tada T, Torii R, Hosoi Y, Kobayashi K, Imahie H, Kondo Y, Iritani A, Nakatsuji N. Establishment of embryonic stem

cell lines from cynomolgus monkey blastocysts produced by IVF or ICSI. *Dev. Dyn.*, **222**, 273–279 (2001).
5) Ginis I, Luo Y, Miura T, Thies S, Brandenberger R, Gerecht-Nir S, Amit M, Hoke A, Carpenter MK, Itskovitz-Eldor J, Rao MS. Differences between human and mouse embryonic stem cells. *Dev. Biol.*, **269**, 360–380 (2004).
6) Suemori H, Nakatsuji N. Generation and characterization of monkey embryonic stem cells. *Methods Mol. Biol.*, **329**, 81–89 (2006).
7) Momose Y, Matsunaga T, Murai K, Takezawa T, Ohmori S. Differentiation of monkey embryonic stem cells into hepatocytes and mRNA expression of cytochrome p450 enzymes responsible for drug metabolism: comparison of embryoid body formation conditions and matrices. *Biol. Pharm. Bull.*, **32**, 619–626 (2009).
8) Lavon N, Benvenisty N. Study of hepatocyte differentiation using embryonic stem cells. *J. Cell. Biochem.*, **96**, 1193–1202 (2005).
9) Asahina K, Fujimori H, Shimizu-Saito K, Kumashiro Y, Okamura K, Tanaka Y, Teramoto K, Arii S, Teraoka H. Expression of the liver-specific gene Cyp7a1 reveals hepatic differentiation in embryoid bodies derived from mouse embryonic stem cells. *Genes Cells*, **9**, 1297–1308 (2004).
10) Heo J, Factor VM, Uren T, Takahama Y, Lee JS, Major M, Feinstone SM, Thorgeirsson SS. Hepatic precursors derived from murine embryonic stem cells contribute to regeneration of injured liver. *Hepatology*, **44**, 1478–1486 (2006).
11) Watanabe K, Ueno M, Kamiya D, Nishiyama A, Matsumura M, Wataya T, Takahashi JB, Nishikawa S, Nishikawa S, Muguruma K, Sasai Y. A ROCK inhibitor permits survival of dissociated human embryonic stem cells. *Nat. Biotechnol.*, **25**, 681–686 (2007).
12) Takehara T, Teramura T, Onodera Y, Kakegawa R, Fukunaga N, Takenoshita M, Sagawa N, Fukuda K, Hosoi Y. Rho-associated kinase inhibitor Y-27632 promotes survival of cynomolgus monkey embryonic stem cells. *Mol. Hum. Reprod.*, **14**, 627–634 (2008).
13) Nishimura M, Koeda A, Suganuma Y, Suzuki E, Shimizu T, Nakayama M, Satoh T, Narimatsu S, Naito S. Comparison of inducibility of CYP1A and CYP3A mRNAs by prototypical inducers in primary cultures of human, cynomolgus monkey, and rat hepatocytes. *Drug Metab. Pharmacokinet.*, **22**, 178–186 (2007).
14) Ohtsuka T, Yoshikawa T, Kozakai K, Tsuneto Y, Uno Y, Utoh M, Yamazaki H, Kume T. Alprazolam as an *in vivo* probe for studying induction of CYP3A in cynomolgus monkeys. *Drug Metab. Dispos.*, **38**, 1806–1813 (2010).
15) Hamazaki T, Iiboshi Y, Oka M, Papst PJ, Meacham AM, Zon LI, Terada N. Hepatic maturation in differentiating embryonic stem cells *in vitro*. *FEBS Lett.*, **497**, 15–19 (2001).
16) Chinzei R, Tanaka Y, Shimizu-Saito K, Hara Y, Kakinuma S, Watanabe M, Teramoto K, Arii S, Takase K, Sato C, Terada N, Teraoka H. Embryoid-body cells derived from a mouse embryonic stem cell line show differentiation into functional hepatocytes. *Hepatology*, **36**, 22–29 (2002).
17) Maezawa K, Miyazato K, Matsunaga T, Momose Y, Imamura T, Johkura K, Sasaki K, Ohmori S. Expression of cytochrome P450 and transcription factors during *in vitro* differentiation of mouse embryonic stem cells into hepatocytes. *Drug Metab. Pharmacokinet.*, **23**, 188–195 (2008).
18) Doetschman TC, Eistetter H, Katz M, Schmidt W, Kemler R. The *in vitro* development of blastocyst-derived embryonic stem cell lines: formation of visceral yolk sac, blood islands and myocardium. *J. Embryol. Exp. Morphol.*, **87**, 27–45 (1985).
19) Cai J, Zhao Y, Liu Y, Ye F, Song Z, Qin H, Meng S, Chen Y, Zhou R, Song X, Guo Y, Ding M, Deng H. Directed differentiation of human embryonic stem cells into functional hepatic cells. *Hepatology*, **45**, 1229–1239 (2007).
20) Agarwal S, Holton KL, Lanza R. Efficient differentiation of functional hepatocytes from human embryonic stem cells. *Stem Cells*, **26**, 1117–1127 (2008).
21) Hay DC, Zhao D, Fletcher J, Hewitt ZA, McLean D, Urruticoechea-Uriguen A, Black JR, Elcombe C, Ross JA, Wolf R, Cui W. Efficient differentiation of hepatocytes from human embryonic stem cells exhibiting markers recapitulating liver development *in vivo*. *Stem Cells*, **26**, 894–902 (2008).
22) Touboul T, Hannan NR, Corbineau S, Martinez A, Martinet C, Branchereau S, Mainot S, Strick-Marchand H, Pedersen R, Di Santo J, Weber A, Vallier L. Generation of functional hepatocytes from human embryonic stem cells under chemically defined conditions that recapitulate liver development. *Hepatology*, **51**, 1754–1765 (2010).
23) Zhou M, Li P, Tan L, Qu S, Ying QL, Song H. Differentiation of mouse embryonic stem cells into hepatocytes induced by a combination of cytokines and sodium butyrate. *J. Cell. Biochem.*, **109**, 606–614 (2010).
24) Sellem CH, Frain M, Erdos T, Sala-Trepat JM. Differential expression of albumin and alpha-fetoprotein genes in fetal tissues of mouse and rat. *Dev. Biol.*, **102**, 51–60 (1984).
25) Sakuma T, Hieda M, Igarashi T, Ohgiya S, Nagata R, Nemoto N, Kamataki T. Molecular cloning and functional analysis of cynomolgus monkey CYP1A2. *Biochem. Pharmacol.*, **56**, 131–139 (1998).
26) Schweikl H, Taylor JA, Kitareewan S, Linko P, Nagorney D, Goldstein JA. Expression of CYP1A1 and CYP1A2 genes in human liver. *Pharmacogenetics*, **3**, 239–249 (1993).
27) Uehara S, Murayama N, Nakanishi Y, Zeldin DC, Yamazaki H, Uno Y. Immunochemical detection of cytochrome P450 enzymes in liver microsomes of 27 cynomolgus monkeys. *J. Pharmacol. Exp. Ther.*, **339**, 654–661 (2011).
28) Iwasaki K, Uno Y. Cynomolgus monkey CYPs: a comparison with human CYPs. *Xenobiotica*, **39**, 578–581 (2009).
29) Kim S, Dinchuk JE, Anthony MN, Orcutt T, Zoeckler ME, Sauer MB, Mosure KW, Vuppugalla R, Grace JE Jr, Simmermacher J, Dulac HA, Pizzano J, Sinz M. Evaluation of cynomolgus monkey pregnane X receptor, primary hepatocyte, and *in vivo* pharmacokinetic changes in predicting human CYP3A4 induction. *Drug Metab. Dispos.*, **38**, 16–24 (2010).

Eur J Clin Pharmacol (2013) 69:21–30
DOI 10.1007/s00228-012-1315-5

PHARMACOGENETICS

The effect of *carboxylesterase 1* (*CES1*) polymorphisms on the pharmacokinetics of oseltamivir in humans

Yuki Suzaki · Naoto Uemura · Makoto Takada · Tetsuji Ohyama · Akiko Itohda · Takuya Morimoto · Hiromitsu Imai · Hajime Hamasaki · Akihiro Inano · Masakiyo Hosokawa · Masato Tateishi · Kyoichi Ohashi

Received: 27 December 2011 / Accepted: 14 May 2012 / Published online: 7 June 2012

Abstract
Purpose The aim of this study was to examine whether *carboxylesterase 1* (*CES1A*) genetic polymorphisms affect the pharmacokinetics of oseltamivir.
Methods Thirty healthy Japanese male and female subjects ranging in age from 20 to 36 years voluntarily participated in this study. These subjects were administered a single 75-mg dose of oseltamivir (Tamiflu®), and blood samples were collected predose and up to 24 h after oseltamivir administration. Oseltamivir and its active metabolite, oseltamivir carboxylate, were measured by liquid chromatography–time of flight/mass spectrometry with solid-phase extraction. The *CES1A* diplotypes [a combination of haplotypes A (*CES1A3-CES1A1*), B (*CES1A2-CES1A1*), C (*CES1A3-CES1A1variant*), and D (*CES1A2-CES1A1variant*)] were determined by PCR-restriction fragment length polymorphism analysis and direct sequencing.
Results All subjects completed the study according to the protocol, and no clinically meaningful adverse events were attributable to the administration of oseltamivir. No significant differences in the pharmacokinetic parameters of oseltamivir and oseltamivir carboxylate were observed according to *CES1A* genotype. In one subject, the peak concentration and area under the concentration–time curve (AUC) of oseltamivir were approximately tenfold higher than the mean values of the other subjects.
Conclusions In our study, the known interindividual variability in oseltamivir metabolism was not explained by *CES1A* genetic polymorphisms, but are likely the result of

This study was registered in the University Hospital Medical Information (UMIN) clinical trials registry (CTR) of Japan under number: UMIN000003774

Y. Suzaki (✉) · T. Ohyama · T. Morimoto · H. Imai · K. Ohashi
General Clinical Research Center, Oita University Hospital,
1-1 Idaigaoka,
Hasama-machi, Yufu-shi, Oita 879-5593, Japan
e-mail: ysuzaki@oita-u.ac.jp

T. Morimoto · H. Imai · H. Hamasaki · K. Ohashi
Clinical Pharmacology Center, Oita University Hospital,
Hasama-machi, Yufu-shi, Oita, Japan

N. Uemura
Department of Pharmaceutical Medicine and Communication,
Oita University Faculty of Medicine,
Yufu-shi, Oita, Japan

A. Itohda · H. Imai · H. Hamasaki · K. Ohashi
Department of Clinical Pharmacology & Therapeutics,
Oita University Faculty of Medicine,
Yufu-shi, Oita, Japan

T. Ohyama
Department of Statistics, Oita University Faculty of Medicine,
Yufu-shi, Oita, Japan

M. Takada · M. Tateishi
Division of Biopharmaceutics, Faculty of Pharmaceutical Sciences, Nagasaki International University,
Sasebo, Nagasaki, Japan

A. Inano
Clinical Research Center, Fukushima Medical University Hospital,
Fukushima, Fukushima, Japan

M. Hosokawa
Laboratory of Drug Metabolism and Biopharmaceutics,
Chiba Institute of Science,
Choshi, Chiba, Japan

other factors. While one subject was found to exhibit an approximate tenfold higher AUC than the other subjects, no abnormal behaviors were associated with the increased oseltamivir plasma concentrations. Further studies are required to reveal the cause of individual differences in CES1A metabolism and the abnormal behavioral effects of oseltamivir.

Keywords Carboxylesterase · CES1 · Oseltamivir · Genetic polymorphism

Introduction

Oseltamivir phosphate (oseltamivir, Tamiflu®) is an ester prodrug which is rapidly converted in vivo into oseltamivir carboxylate, an active neuraminidase inhibitor, and is widely used for the treatment of influenza virus A and B infections [1, 2]. The conversion of oseltamivir into oseltamivir carboxylate is mediated by hepatic carboxylesterase (CES) 1 [3]. The interindividual variability in the expression of CES1 may affect the efficacy of oseltamivir.

CES hydrolyzes drugs and chemicals containing such functional groups as carboxylic acid esters, amides, and thioesters. It plays an important role in drug metabolism by activating prodrugs and is also involved in insecticide detoxification [4–8]. The mammalian CES represents a multi-gene family of isozymes that have been classified into four main groups (CES1–CES4) and several subgroups based on the homology of the amino acid sequence [7]. CES1 and CES2 are the two major human CES families present in human tissues. CES1 is expressed at high levels in the liver and the lung but at low levels in the intestine, and its primary action is the hydrolysis of substrates with a small alcohol group and a large acyl group. In comparison, CES2 is highly expressed in the intestine and kidney but shows low expression in the liver and lung; its primary action is the hydrolysis of substrates with a large alcohol group and a small acyl group [5, 7]. The human *CES1* gene family consists of two functional genes, *CES1A1* and *CES1A2*, each of which contains 14 exons encoding 567 amino acids. These two genes show 98 % homology and differ only by five nucleotides (4 amino acids) in exon 1, which encodes a signal peptide [5, 7]. In addition, both genes are reported to be located tail-to-tail on chromosome 16q13-q22.1 (Fig. 1) [9]. A *CES1A1variant* (*1A1variant*) has recently been identified in which exon 1 was replaced by exon 1 of *CES1A2*. The *CES1* gene family also contains a pseudogene, *CES1A3* (formerly recognized as *CES4*). The sequence of this pseudogene from the promoter region to exon 1 is the same as that of *CES1A2*, but it contains a stop codon in exon 3 [10, 11]. *CES1* is represented by four haplotypes: A (*CES1A3-CES1A1*), B (*CES1A2-CES1A1*), C (*CES1A3-CES1A1variant*), and D (*CES1A2-CES1A1variant*) [11] (Fig. 1). The mature proteins are produced from *CES1A1*, *1A1variant*, and *CES1A2*. Moreover, humans can have a maximum of four functional *CES1* genes through a combination of haplotypes A–D. The CES1A1 mRNA is transcribed from the *CES1A1* gene, whereas the CES1A2 mRNA is transcribed from both the *1A1variant* and *CES1A2* genes [11]. The promoter activity of the *CES1A2* gene is significantly lower than that of the *CES1A1* gene based on in vitro data from a luciferase assay in hepatoma cell line [10]. CES1A1 mRNA levels appear to be higher than those of CES1A2 mRNA, and the levels of CES1A2 mRNA transcribed from the *CES1A2* gene are substantially lower than those transcribed from *1A1variant* [11]. As predicted for a pseudogene, CES1A3 mRNA has not been detected in human liver samples [11]. It is not yet known just how polymorphisms of the *CES1* genes affect the in vivo expression of CES1 in humans, but differences in CES1 activity may alter the pharmacokinetics of CES1 substrates, including marketed prodrugs.

Abnormal behavior (neuropsychiatric events—including delirium, convulsions, and encephalitis) has recently been reported in children with influenza who were administered oseltamivir, and both oseltamivir and oseltamivir carboxylate have been shown to have neuroexcitatory actions in the central nervous system (CNS) [12]. However, the relationship between the reported abnormal behaviors and oseltamivir medication has not yet been elucidated. Interindividual differences in the metabolic rate (pharmacokinetics) of drugs are often significantly related to the expression of the side effects associated with the particular drug. At the present time, no clinical data are available to enable clarification of whether or not *CES1* polymorphisms affect the pharmacokinetics of oseltamivir. Thus, this study was designed to examine whether the pharmacokinetics of oseltamivir is affected by *CES1A* genetic polymorphisms.

Methods

Materials

For the purpose of this study, we purchased 75-mg capsules of oseltamivir (Tamiflu®) (as a 98-mg phosphate salt) from Chugai Pharmaceutical Company (Tokyo, Japan). Oseltamivir phosphate, its active metabolite oseltamivir carboxylate, oseltamivir phosphate salt threefold deuterated drug (OP-d3), and oseltamivir carboxylate threefold deuterated drug (OC-d3) were gifts from F. Hoffmann-La Roche (Basel, Switzerland). Ethanol, methanol, formic acid, and dihydrogen phosphate [Lichrosolv for high-performance liquid chromatography (HPLC)] were obtained from Wako Pure Chemical Industries (Osaka, Japan). The Blend Taq DNA polymerase was purchased from Toyobo (Tokyo, Japan),

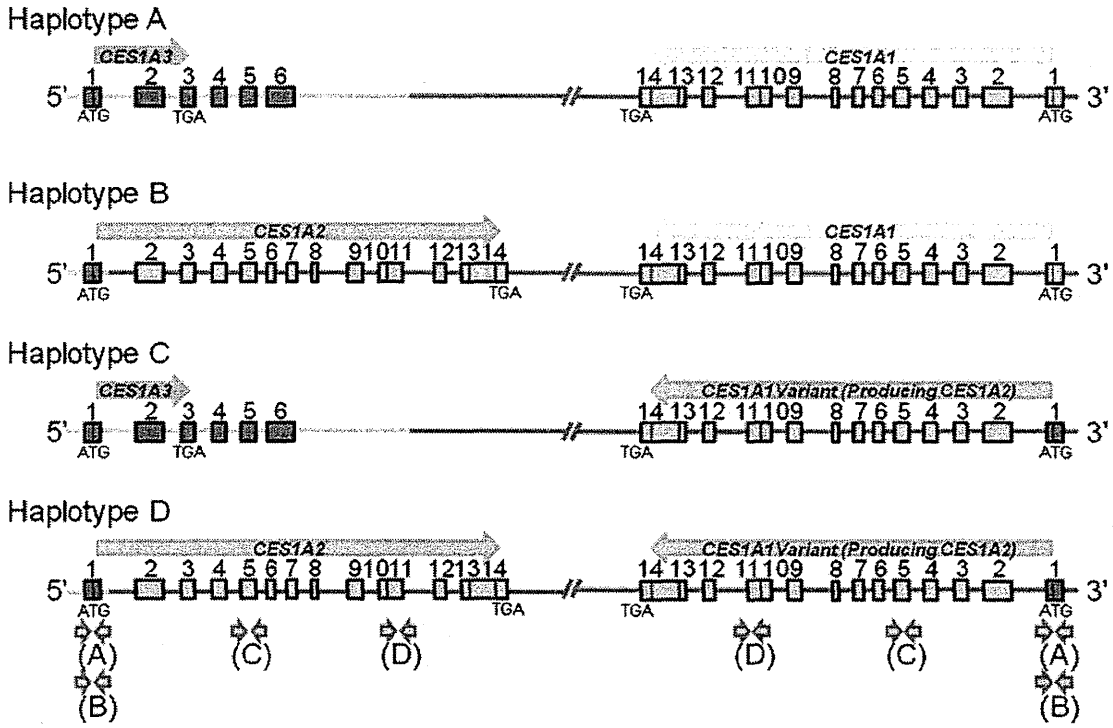

Fig. 1 Carboxylesterase 1 (*CES1*) gene structure and haplotypes. For haplotypes A–D, the region used for haplotype determination is indicated with *arrows*

and restriction enzymes were purchased from New England BioLabs Japan (Tokyo, Japan). Primers were commercially synthesized at Sigma-Aldrich Japan (Tokyo, Japan). The MinElute column, the AutoSeq G-50 column, and the ABI BigDye Terminator Cycle Sequencing kit were obtained from Qiagen (Hilden, Germany), GE Healthcare (Buckinghamshire, UK), and Applied Biosystems (Foster City, CA), respectively. All other chemicals and solvents were of the highest grade commercially available.

Clinical trial

The clinical trial was performed as an open-label study and was conducted in the Clinical Trial Unit of Oita University Hospital. This study was approved by the Institutional Review Board of Oita University Hospital. The use of genomic DNA was approved by the Ethics Committee of Oita University Faculty of Medicine. The Japanese male and female subjects who participated in the trial provided written informed consent. These subjects were ascertained to be healthy on the basis of their medical history, a physical examination, an electrocardiogram, whole blood cell counts, serum chemical analysis, and urinalysis. The subjects were nonsmokers and were not taking any medication. Moreover, they were asked not to consume any grapefruit-containing beverages or St. John's Wort-containing supplements within 1 week of the drug administration and not to drink alcohol or caffeine-containing beverages 1 day before receiving the drug. A total of 30 Japanese subjects, between 20–36 years of age, were administered a single dose of a 75-mg capsule of oseltamivir with 200 mL of water under fasting conditions. Blood samples were collected predose and at 0.25, 0.5, 0.75, 1, 1.5, 2, 3, 4, 5, 6, 8, 10, 12, and 24 h after post-oseltamivir administration. The blood samples were collected in heparinized tubes and centrifuged at 3,000 rpm for 10 min; plasma samples were stored at −20°C until oseltamivir and oseltamivir carboxylate levels were analyzed. The safety of a single dose of oseltamivir was evaluated by the following items: adverse events, vital signs, and visual analog self-rating scales (VAS). Subjects were evaluated for the CNS effect of oseltamivir by *CES1A* genotype groups using a 100-mm VAS that included "feeling disoriented," "feeling drowsiness," "stress level," "level of excitement," "level of emotional stress," and "fatigue." The VAS was administered predose and at 1, 2, 4, 6, 12, and 24 h post-oseltamivir administration. All post-dose values were expressed as the change in VAS from predose baseline, and the area under the score–time curve adjusted by baseline (VAS-AUC) was determined by the trapezoidal rule from 0 to 24 h.

Determination of the *CES1* genotype

Genomic DNA was extracted from the blood samples of the volunteers using DNA isolation system (TOYOBO) to investigate the diplotypes of the *CES1A* genes. The diplotypes

of *CES1A* genes were determined with the polymerase chain reaction (PCR). *CES1A1* and *1A1variant* were discriminated by restriction fragment length polymorphism (RFLP) analysis for exon 1, as described in Fukami et al.[11], and by sequencing exon 1 and the flanking region, as reported in Sai et al. [13] (Fig. 1 (a) (b)).

CES1A2 and *CES1A3* were discriminated by PCR-RFLP analysis of exons 5 and 11, as described in a previous report [11] (Fig. 1 (©) (d)). The copy number of *CES1A3* (0, 1, or 2) was confirmed by direct sequencing of exon 5 using the same primer set reported by Sai et al. [13].

Determination of oseltamivir and oseltamivir carboxylate concentrations

Oseltamivir and oseltamivir carboxylate were measured by liquid chromatography–time of flight/mass spectrometry (LC-TOF/MS) (JMS-T100LP; JEOL, Tokyo, Japan) with solid-phase extraction using a modification of the method of Heinig and Bucheli [14]. Briefly, a 500 μL aliquot of each plasma sample was mixed with 500 μL of MeOH and an internal standard solution (IS) (50 ng/mL of OP-d3 and 50 ng/mL of OC-d3), then vortexed and centrifuged at 5,000 rpm for 10 min. The sample mixture separated into a MeOH layer (I) and a residue. The residue was added to MeOH (500 μL) and vortexed and centrifuged at 5,000 rpm for 10 min. The residue once again separated into a MeOH layer (II) and a residue. The MeOH layers (I) and (II) were mixed together and then added to 10 mL of H_2O and 1 mL of H_3PO_4. Oasis HLB columns were prepared with 1 mL of MeOH and 1 mL of H_2O. The samples were added into Waters Oasis HLB columns (60 mg; Waters, Milford, MA) and eluted with 2 mL MeOH. The sample extract was concentrated under a gentle nitrogen stream, and the concentrated sample was then added to 50 % MeOH and the volume adjusted to a final volume of 500 μL. The samples were applied into the LC-TOF/MS system consisting of Waters Atlantis T3 HPLC analytical columns (3.5 μm, 2.1 × 50 mm; Waters). The calibration curve was prepared by adding IS and oseltamivir or oseltamivir carboxylate in MeOH to control plasma to obtain final concentrations of 1.0–1,000 ng/mL oseltamivir and 5.0–1000 ng/mL oseltamivir carboxylate. Linear regression analysis of the ratio of the area of the analyte to that of IS versus the concentration was used for calibration purposes. A good linearity was obtained (coefficient of determination in the oseltamivir range of 1 to 1,000 ng/mL was $r^2 \geq 0.9999$; that in the oseltamivir carboxylate range of 5 to 1,000 ng/mL was $r^2 = 1.00$).

An Agilent HPLC system with a Walters analytical column (T3; 3.5 μm, 2.1 × 50 mm) was used, and 10 μL samples were injected automatically. Solvent A (0.1 % formic acid in distilled water) and solvent B (0.1 % formic acid in methanol) were used as mobile phases for gradient elution (gradient curve: 0 min, 5 % B; 0–8 min, linear change from 5 to 95 % B; 8–12 min, 95 % B; run time 16 min). The flow rate was set at 0.5 mL/min. A TOF/MS with an electro-spray ionization interface (JEOL) was used, and detection was performed by monitoring the positive ions. The theoretical m/z values of [M+H]+ion were 313.1 and 285.1 for oseltamivir and oseltamivir carboxylate, respectively.

Pharmacokinetic analysis

The pharmacokinetic parameters of oseltamivir and oseltamivir carboxylate were determined by noncompartmental analysis using WinNonlin Professional (ver 5.2; Pharsight Co, Mountain View, CA). The Log-linear trapezoidal method with extrapolation to infinite time was used to calculate the area under the plasma concentration–time curve ($AUC_{(0,\infty)}$). The terminal elimination half-life ($T_{1/2}$) was calculated by ln2/lambda *z*, where lambda *z* is the terminal slope calculated by the linear regression of the time versus log concentration. Apparent oral clearance (CL/F) was calculated by Dose/$AUC_{(0,\infty)}$. In addition, the AUC ratio of oseltamivir carboxylate to oseltamivir ($[AUC_{oseltamivir\ carboxylate}]/[AUC_{oseltamivir}]$) was used as a parameter for the in vivo CES1 activity. The oseltamivir and oseltamivir carboxylate levels were monitored by the LC-TOF/MS system. Pharmacokinetic parameters in subjects were analyzed for each group on the basis of the number of *CES1* functional genes and *CES1A1* genotype.

Statistical analysis

Statistical analysis was performed with SPSS for Windows (ver 16.0 J; SPSS, Tokyo, Japan). With the exceptions of T_{max} and the in vivo CES1 activity, the data are expressed as geometric means and coefficient of variations. The time after the administration of oseltamivir when the maximum plasma concentration was reached (T_{max}) was expressed as median, minimum, and maximum values. All pharmacokinetic variables, except for T_{max}, were log-transformed, the linear regression models were adjusted for the *CES1A1* genotype, and the functional gene number was used to estimate and compare means. Differences in T_{max} and the in vivo CES1 activity between the *CES1A1* genotypes were examined using the Kruskal–Wallis test. Differences in T_{max} and the in vivo CES1 activity between genotypes with different functional gene numbers were analyzed using the Mann–Whitney *U* test. The differences in all pharmacokinetic parameters, except for T_{max}, between males and females were log-transformed and compared by the two-sample *t* test. Differences in T_{max} between males and females were examined using the Mann–Whitney *U* test. The VAS-AUC was analyzed using the linear regression

model adjusted for the *CES1A1* genotype. A $p<0.05$ was considered to be statistically significant.

Results

Characteristics of the participants

All subjects completed the study according to the protocol, and no clinically meaningful adverse events were attributable to the administration of oseltamivir. In particular, no meaningful effect on CNS activity was detected in the subjects following the single-dose administration of 75 mg oseltamivir. There were no significant differences in the VAS-AUC between the different *CES1A1* genotypes [feeling disoriented (p=0.284), feeling drowsiness (p=0.348), stress level (p = 0.883), level of excitement (p=0.776), level of emotional stress (p=0.867), and fatigue (p=0.455)]. The subjects were then categorized according to *CES1A* genotype and the functional gene number (Table 1). The frequencies of *CES1A1* and *1A1variant* were 0.733 and 0.267, respectively, and those of *CES1A2* and *CES1A3* were 0.600 and 0.400, respectively. The frequency of two, three, and four copies of functional *CES1* genes was 0.000, 0.800, and 0.200, respectively.

After the single 75-mg oral administration of oseltamivir, the pharmacokinetic parameters of oseltamivir and oseltamivir carboxylate were not significantly different by gender [oseltamivir: T_{max}, (p=0.964), C_{max}, (p=0.508), $T_{1/2}$ (p= 0.168), CL/F (p =0.142), $AUC_{(0,\infty)}$ (p=0.142), Vd/F (p = 0.581), MRT (p=0.451); oseltamivir carboxylate: T_{max} (p= 0.631), C_{max} (p=0.329), $T_{1/2}$ (p=0.814), CL/F (p=0.251), $AUC_{(0,\infty)}$ (p=0.074), Vd/F (p=0.074), MRT (p=0.961)]. However, we found a subject with C_{max} and AUC values for oseltamivir that were approximately tenfold higher than the mean values for these parameters in the other subjects. The $T_{1/2}$ and CL/F values for oseltamivir in this participant were markedly longer and lower, respectively, than those in the other individuals (Table 2), while the AUC, $T_{1/2}$, and C_{max} values for oseltamibir carboxylate were substantially lower than the mean values for these parameters in the other subjects (Table 3). The median AUC ratio ($[AUC_{oseltamivir\ carboxylate}]/[AUC_{oseltamivir}]$) as shown by the in vivo CES1 activity was also significantly lower in this subject (Fig. 4). The diplotypes of this subject was B/C, and the number of functional genes was three. Because this subject represented an outlier, the data pertaining to this subject were excluded from the statistical analysis.

Assessment according to *CES1A1* genotype

The differences in oseltamivir metabolism were evaluated according to *CES1A1* genotype by separating the subjects into three groups: *CES1A1/1A1*, *CES1A1/1A1variant*, and *1A1variant/1A1variant*. No significant differences in the pharmacokinetic parameters of oseltamivir were observed between the *CES1A* genotypic groups (Fig. 2; Table 2). The plasma concentration–time profiles of oseltamivir for the *1A1variant/ 1A1variant* genotype showed a bimodal peak because each T_{max} was in the range of 0.5–2.0 h (Fig. 2). Moreover, some subjects in all groups showed a double peak phenomenon and/ or T_{max} delay. No significant differences in the pharmacokinetic parameters of oseltamivir carboxylate were observed between the different genotypes (Fig. 3; Table 2).

Assessment based on the functional gene number of *CES1A*

The differences in oseltamivir metabolism based on the number of *CES1* functional genes were evaluated. The

Table 1 Frequency of *CES1* genes and diplotypes in Japanese healthy subjects

CES1 diplotype	Number of *CES1* functional genes				Total number of functional genes	Number of subjects (male/female)	Frequency (n=30)	
	1A1	*1A1variant*	*1A2*	*1A3*			Per diplotype	Mean
A/A	2	0	0	2	2	0	0.000	0.00
A/C	1	1	0	2		0	0.000	
C/C	0	2	0	2		0	0.000	
A/B	2	0	1	1	3	14 (7/7)	0.467	0.80
A/D or B/C	1	1	1	1		7 (6/1)	0.233	
C/D	0	2	1	1		3 (1/2)	0.100	
B/B	2	0	2	0	4	4 (1/3)	0.133	0.20
B/D	1	1	2	0		1 (1/0)	0.033	
D/D	0	2	2	0		1 (0/1)	0.033	
Frequency (n=30)	0.733	0.267	0.600	0.400				

CES1, Carboxylesterase 1 gene

The functional genes are *CES1A1*, *1A1variant*, and *1A2*

Table 2 Pharmacokinetic parameters of oseltamivir

Oseltamivir	T_{max} (h)	C_{max} (ng/mL)	$T_{1/2}$ (h)	CL/F (L/h)	$AUC_{(0,\infty)}$ (h ng/mL)	Vd/F (L)	MRT (h)
CES1A1 genotype							
1A1/1A1	0.75	87.36	1.78	367.1	204.3	945.1	3.05
(*n* =18)	(0.50, 5.00)	(51.65, 147.76)	(1.05, 3.02)	(217.0, 621.0)	(120.8, 345.6)	(558.8, 1598.6)	(1.80, 5.16)
1A1/1A1variant	1.00	84.24	1.70	437.1	171.6	1071.0	3.05
(*n*=7)	(0.50, 5.00)	(37.55, 188.95)	(0.76, 3.81)	(194.8, 980.4)	(76.5, 384.9)	(477.5, 2402.3)	(1.36, 6.84)
1A1variant/1A1variant	1.375	120.41	1.30	437.1	229.7	613.3	2.38
(*n*=4)	(0.50, 2.00)	(44.05, 329.15)	(0.48, 3.56)	(194.8, 980.4)	(84.0, 627.8)	(224.4, 1676.5)	(0.87, 6.51)
p value	0.500	0.825	0.850	0.884	0.884	0.661	0.900
Functional gene number							
Functional gene 3	0.75	94.37	1.41	404.5	185.4	820.4	2.45
(*n*=23)	(0.50, 2.00)	(58.69, 151.75)	(0.87, 2.26)	(251.5, 650.4)	(115.3, 298.2)	(510.2, 1319.3)	(1.52, 3.93)
Functional gene 4	2.50	97.75	1.78	346.2	216.7	887.0	3.22
(*n*=6)	(0.50, 5.00)	(42.19, 226.48)	(0.77, 4.11)	(149.4, 802.0)	(93.5, 502.0)	(382.8, 2055.0)	(1.39, 7.47)
p value	0.005	0.939	0.612	0.735	0.735	0.865	0.549
Outlier							
(*n*=1)	0.50	940.83	3.53	25.47	2944.07	129.83	5.70

T_{max}, Time to reach the maximum plasma concentration; C_{max}, maximum plasma concentration; $T_{1/2}$, terminal elimination half-life; CL/F, apparent oral clearance; $AUC_{(0,\infty)}$, area under the plasma concentration–time curve from time 0 to infinity; Vd/F, apparent oral volume of distribution; MRT, mean residence time

Except for T_{max}, the data are expressed as geometric means with the values in parentheses representing the 95 % confidence intervals (CI). T_{max} is expressed as the median, minimum, and maximum values (with the latter two values in parenthesis)

subjects were separated into three groups based on whether individuals possessed two, three, or four functional gene copies. In this study, no subjects were found to carry only two functional gene copies. No significant differences in the

Table 3 Pharmacokinetic parameters of oseltamivir carboxylate

Oseltamivir carboxylate	T_{max} (h)	C_{max} (ng/mL)	$T_{1/2}$ (h)	CL/F (L/h)	$AUC_{(0,\infty)}$ (h ng/mL)	Vd/F (L)	MRT (h)
CES1A1 genotype							
1A1/1A1	5.0	557.0	6.53	11.62	6452.6	109.5	11.61
(*n*=18)	(3.0, 6.0)	(329.3, 942.1)	(3.86, 11.04)	(6.87, 19.66)	(3814.8, 10914)	(64.7, 185.2)	(6.86, 19.63)
1A1/1A1variant	4.0	578.1	5.58	13.65	5493.7	109.8	9.83
(*n*=7)	(1.5, 6.0)	(257.7, 1296.6)	(2.49, 12.51)	(6.09, 30.62)	(2449.2, 12323)	(49.0, 246.4)	(4.38, 22.05)
1A1variant/1A1variant	4.0	735.1	4.66	11.44	6557.6	76.8	8.52
(*n*=4)	(3.0, 6.0)	(268.9, 2009.5)	(1.70, 12.73)	(4.18, 31.26)	(2398.9, 17926)	(28.1, 210.0)	(3.12, 23.30)
p value	0.230	0.881	0.809	0.931	0.931	0.805	0.829
Functional gene number							
Functional gene 3	5.0	637.2	5.12	11.86	6325.9	87.5	9.23
(*n*=23)	(1.5, 6.0)	(396.3, 1024.6)	(3.18, 8.23)	(7.37, 19.06)	(3934.0, 10172)	(54.4, 140.7)	(5.74, 14.85)
Functional gene 4	6.0	600.5	5.99	12.55	5976.4	108.4	10.63
(*n*=6)	(3.0, 6.0)	(259.2, 1391.3)	(2.58, 13.87)	(5.42, 29.07)	(2579.5, 13846)	(46.8, 251.2)	(4.59, 24.63)
p value	0.522	0.898	0.733	0.902	0.902	0.642	0.759
Outlier							
(*n*=1)	5.0	252.61	6.0	24.62	2785.54	213.30	11.08

Except for T_{max}, the data are expressed as geometric means with the values in parentheses representing the 95 % confidence intervals (CI). T_{max} is expressed as the median, minimum, and maximum values (with the latter two values in parenthesis)

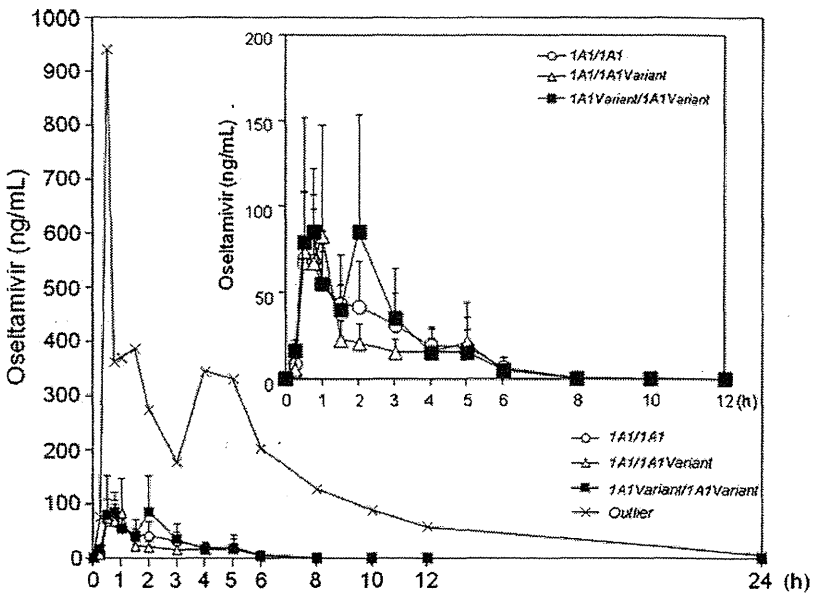

Fig. 2 Plasma concentration–time profile of oseltamivir for the *CES1A1* genotype after oseltamivir administration. Each value represents the mean± standard deviation (SD). *Open circle CES1A1/1A1* (n=18), *open triangle CES1A1/1A1variant* (n=7), *filled square 1A1variant/1A1variant* (n=4), *X* outlier (n=1)

pharmacokinetic parameters of oseltamivir or oseltamivir carboxylate were observed on the basis of the *CES1A* functional gene copy number (Tables 2; 3).

Evaluation of in vivo *CES1* activity

The AUC ratio of oseltamivir carboxylate to oseltamivir was used to assess individual variability in the ability to metabolize oseltamivir into oseltamivir carboxylate (Fig. 4). The median AUC ratio of individuals with *CES1A1/1A1*, *CES1A1/1A1variant*, and *1A1variant/1A1variant* were [median (25th–75th percentiles)] 33.16 (26.40–39.59), 36.32 (28.61–39.59), and 27.17 (26.06–32.32) (p=0.652), respectively. The median AUC ratio of the *CES1A1/1A1* and *CES1A1/1A1variant* groups was 1.22- and 1.34-fold higher, respectively, than that of the *1A1variant/1A1variant* group (p=0.396 and p=0.257, respectively). The median AUC ratio of three and four functional gene copies was [median (25th–75th percentiles)] 34.97 (27.17–42.63) and 27.68 (25.84–29.77) (p=0.146), respectively. The median AUC ratio of four functional gene copies was 1.26-fold smaller than that of three functional gene copies. No significant differences were observed between *CES1A1* and *CES1A1variant* (among *CES1A1/1A1*, *CES1A1/1A1variant*, and *1A1variant/1A1variant*) and three or four functional gene copies (Fig. 4).

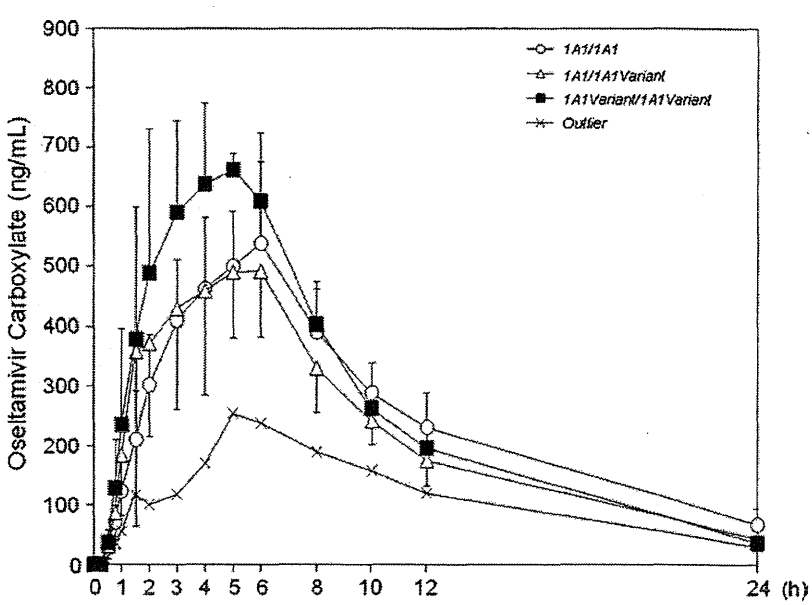

Fig. 3 Plasma concentration–time profile of oseltamivir carboxylate for the *CES1A1* genotype after oseltamivir administration. Each value represents the mean±SD. *Open circle CES1A1/1A1* (n=18), *open triangle CES1A1/1A1variant* (n=7), *filled square 1A1variant/1A1variant* (n=4); *X* outlier (n=1)

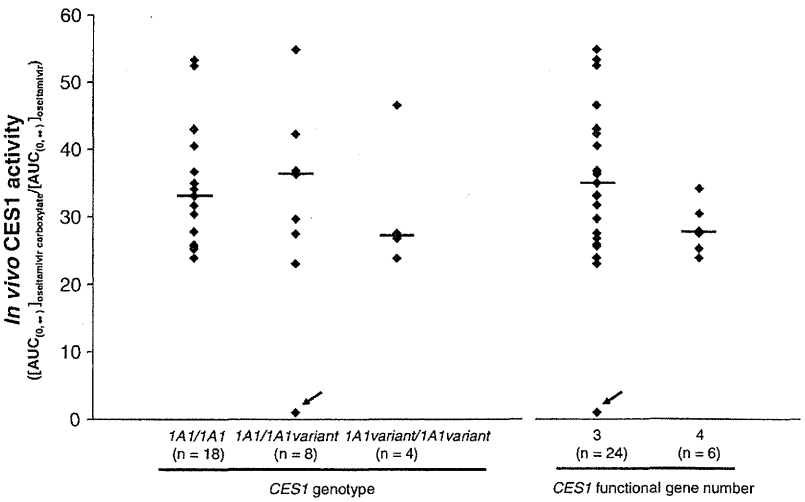

Fig. 4 The in vivo CES1 activity for oseltamivir metabolism. The area under the time–concentration curve ratio of oseltamivir carboxylate to oseltamivir [$AUC_{oseltamivir\ carboxylate}$]/[$AUC_{oseltamivir}$] was shown according to *CES1A* genotype and *CES1* functional gene number. The presence/absence of *CES1A1*, *1A1variant*, and *CES1A2* was used to determine the number of *CES1* functional genes. *Horizontal bars* Median in each group, excluding the outlier, *arrows* indicate outlier

Discussion

In this study, we evaluated the influence of *CES1A* genetic polymorphisms on oseltamivir metabolism by examining the effect of *CES1A* genotypes and functional gene numbers and found that *CES1A* genetic polymorphisms had little influence on the AUC, C_{max}, and other pharmacokinetic parameters of oseltamivir and oseltamivir carboxylate. In one of our subjects, however, the AUC value for oseltamivir was about tenfold higher than the mean value of the other subjects (Fig. 2; Table 2); additionally, the AUC value for oseltamivir carboxylate in this subject was lower than the mean value of the other participants (Fig. 3; Table 3). The diplotypes of this volunteer was B/C, and the number of functional genes was three. This subject showed a low in vivo CES1 activity compared to that of the other subjects, but the mechanism by which this subject achieved this outlier pharmacokinetic profile is not yet clear. However, based on the AUC, C_{max}, $T_{1/2}$, and CL/F data for oseltamivir, the metabolism of oseltamivir, but not oseltamivir carboxylate, was slow in this subject. It is therefore possible that another mutation in the *CES1* gene may be involved in the slow metabolism of oseltamivir in this individual. The frequency of such outliers is not known. Although this subject showed no adverse events in response to the higher exposure to oseltamivir, further research will be required to identify adverse events (e.g., abnormal behaviors), if any, related to the altered pharmacokinetics of oseltamivir in individuals that slowly metabolize oseltamivir.

Species differences are caused by tissue-dependent hydrolase activity mediated by CES, which makes it difficult to predict effectiveness in humans based on a preclinical study using animals [15]. Thus, we conducted our experimental study in humans to evaluate CES activity. Data on human *CES1A* genetic polymorphisms are still limited. The A(-816)C genotype, which is associated with the promoter activity of the gene, has been reported to be involved in the difference in blood pressure reduction caused by imidapril [16]. The -816A>C is the major single nucleotide polymorphism (SNP) of *CES 1A3* but it is very rare in *CES1A2* [13]. The presence, or not, of this SNP on the *CES1A2* or *CES1A3* gene is important because only the *CES1A2* gene encodes a functional enzyme. The imidapril study was not able to explain individual differences in imidapril metabolism since the CES1A mRNA and protein levels and the imidapril hydrolase activity in human liver are not significantly different between carriers of the *CES1A1/1A1* and *1A1variant/1A1variant* [11]. Similarly, Japanese cancer patients with the *CES1A1/1A1*, *CES1A1/1A1variant*, or *1A1variant/1A1variant* showed no significant difference in irinotecan metabolism [13]. In general, these data are consistent with the results of our study. Genetic differences between *CES1A1* and *1A1variant* appeared to have no meaningful effect on in vivo CES1 activity in our subjects. However, the irinotecan study reported that the total number of functional *CES1A* genes could influence the formation of the active metabolite of irinotecan [13]. It also reported that the increase in the median AUC ratio with an increase in the functional gene number from two to three or four was only 20 % and that such alterations might be masked by other non-genetic factors, hepatic and renal function, irinotecan dosage, and smoking history. In our study in which healthy subjects were investigated, factors other than the genetic factors were also strictly controlled. Based on our results, CES1 activity does not appear to be greatly influenced by the number of functional genes. However, we have not completely ruled out the possibility that functional gene number plays a role in determining CES1 activity since all of our subjects had three or four *CES1* functional gene copies, but none had two.

This study has a number of limitations. First, the scale of the trial (n=30) was relatively small. The frequencies of individual *CES1A1* and *1A1variant* genes in the general Japanese study population were found to be 0.748 and 0.252, respectively, in one study [11] and 0.703 and 0.297, respectively, in another study [13]. The frequencies of individual *CES1A1* and *1A1variant* genes in our data were 0.733 and 0.267, respectively. Hence, our data are comparable to those of previous reports on the Japanese general population. The frequencies of *CES1A2* and *CES1A3* in the Japanese general population were 0.313 and 0.687, respectively [11], and 0.336 and 0.664, respectively [13], in these same two studies. In our study, the frequencies of *CES1A2* and *CES1A3* were 0.600 and 0.400, respectively, so that our frequencies are somewhat different from those of these previous reports. Furthermore, in these previous studies, the genetic analysis was performed with 100 or more subjects. The frequencies of Japanese cancer patients with two, three, and four functional *CES1* genes were found to be 0.44, 0.47, and 0.09, respectively [13]; in comparison, these were 0.000, 0.800, and 0.200, respectively, in our study. The small number of participants in our study may have resulted in these differences in the observed frequencies between our study and the two larger studies [11, 13]. We were unable to recognize clinically meaningful differences in the oseltamivir pharmacokinetics by the *CES1A* genetic polymorphism.

Oseltamivir is rapidly hydrolyzed to oseltamivir carboxylate by CES1 in the liver [3] and mostly excreted into the urine by glomerular filtration and active tubular secretion via organic anion transporter 1 without further metabolism [17]. Oseltamivir was recently characterized as a substrate for peptide transporter (PEPT) 1 [18]. The pharmacokinetics of oseltamivir administered by the oral route may be affected by PEPT1 to a relatively greater degree than by other routes because PEPT1 is mainly expressed in the duodenum. A previous study reported that the plasma concentration–time profile of oseltamivir occasionally shows the double-peak phenomenon due to enterohepatic circulation [19]. It has been suggested that the first peak around 1 h after oseltamivir administration is associated with PEPT1 metabolism because the transit time of the duodenum in humans is considered to be about 40 min [20] and that the second peak may reflect absorption through a pathway other than PEPT1 [21]. Genetic polymorphisms have been reported for PEPT1 [22], and the delay in T_{max} may relate these PEPT1 polymorphisms. Furthermore, oseltamivir is a substrate of P-glycoprotein (P-gp) [23], which is expressed in several tissues in the small intestine and kidney. However, oseltamivir carboxylate is also a substrate of organic anion transporter 3 and multidrug resistance-association protein (MRP) 4 [24]—and genetic polymorphisms have also been reported for both P-gp [25] and MRP-4 [26]. The outlier may therefore also involve polymorphisms in the genes encoding these proteins as well as other mutations in the *CES1* gene. In the case of oral administration, these transporters in the intestine may influence drug absorption, metabolism, and elimination. It may be very difficult to explain interindividual variability in the pharmacokinetics of oseltamivir based solely on CES1 activity.

Conclusions

Based on the results obtained in our healthy Japanese volunteers, we were unable to explain individual differences in the metabolism of oseltamivir by the difference in *CES1A* genetic polymorphisms. Moreover, no meaningful differences were found in the oseltamivir pharmacokinetics between *CES1A1/CES1A1* and *1A1variant/1A1variant*. CES1 activity was not different between subjects with three and four functional genes. However, it remains unknown whether oseltamivir metabolism changes in the presence of two functional *CES1* genes compared with three or four functional genes. One subject from among our 30 subjects was an outlier with about a tenfold higher AUC for oseltamivir. No adverse events, including CNS changes or abnormal behaviors, were associated with a single dose of oseltamivir in our study subjects, including in the outlier.

Acknowledgments This study was supported by the Japanese Research Foundation for Clinical Pharmacology and by a 2011 Grant-in-Aid for Young Scientists (B) (Grant no. 23790604) from the Ministry of Education, Science, Sports and Culture. We thank F. Hoffmann-La Roche Ltd (Switzerland) for providing analytical standards of oseltamivir, its metabolites, threefold deuterated oseltamivir, and its metabolites.

Conflict of interest None.

References

1. von Itzstein M, Wu WY, Kok GB, Pegg MS, Dyason JC, Jin B, Van Phan T, Smythe ML, White HF, Oliver SW et al (1993) Rational design of potent sialidase-based inhibitors of influenza virus replication. Nature 363(6428):418–423. doi:10.1038/363418a0
2. Bardsley-Elliot A, Noble S (1999) Oseltamivir. Drugs 58(5):851–860, discussion 861–852
3. Shi D, Yang J, Yang D, LeCluyse EL, Black C, You L, Akhlaghi F, Yan B (2006) Anti-influenza prodrug oseltamivir is activated by carboxylesterase human carboxylesterase 1, and the activation is inhibited by antiplatelet agent clopidogrel. J Pharmacol Exp Ther 319(3):1477–1484. doi:10.1124/jpet.106.111807
4. Satoh T, Hosokawa M (2006) Structure, function and regulation of carboxylesterases. Chem Biol Interact 162(3):195–211. doi:10.1016/j.cbi.2006.07.001
5. Hosokawa M (2008) Structure and catalytic properties of carboxylesterase isozymes involved in metabolic activation of prodrugs. Molecules 13(2):412–431

6. Redinbo MR, Potter PM (2005) Mammalian carboxylesterases: from drug targets to protein therapeutics. Drug Discov Today 10 (5):313–325. doi:10.1016/S1359-6446(05)03383-0
7. Imai T (2006) Human carboxylesterase isozymes: catalytic properties and rational drug design. Drug Metab Pharmacokinet 21 (3):173–185
8. Imai T, Taketani M, Shii M, Hosokawa M, Chiba K (2006) Substrate specificity of carboxylesterase isozymes and their contribution to hydrolase activity in human liver and small intestine. Drug Metab Dispos 34(10):1734–1741. doi:10.1124/dmd.106.009381
9. Hosokawa M, Furihata T, Yaginuma Y, Yamamoto N, Watanabe N, Tsukada E, Ohhata Y, Kobayashi K, Satoh T, Chiba K (2008) Structural organization and characterization of the regulatory element of the human carboxylesterase (CES1A1 and CES1A2) genes. Drug Metab Pharmacokinet 23(1):73–84
10. Tanimoto K, Kaneyasu M, Shimokuni T, Hiyama K, Nishiyama M (2007) Human carboxylesterase 1A2 expressed from carboxylesterase 1A1 and 1A2 genes is a potent predictor of CPT-11 cytotoxicity in vitro. Pharmacogenet Genomics 17(1):1–10. doi:10.1097/01.fpc.0000230110.18957.50
11. Fukami T, Nakajima M, Maruichi T, Takahashi S, Takamiya M, Aoki Y, McLeod HL, Yokoi T (2008) Structure and characterization of human carboxylesterase 1A1, 1A2, and 1A3 genes. Pharmacogenet Genomics 18(10):911–920. doi:10.1097/FPC.0b013e32830b0c5e
12. Izumi Y, Tokuda K, O'Dell KA, Zorumski CF, Narahashi T (2007) Neuroexcitatory actions of Tamiflu and its carboxylate metabolite. Neurosci Lett 426(1):54–58. doi:10.1016/j.neulet.2007.08.054
13. Sai K, Saito Y, Tatewaki N, Hosokawa M, Kaniwa N, Nishimaki-Mogami T, Naito M, Sawada J, Shirao K, Hamaguchi T, Yamamoto N, Kunitoh H, Tamura T, Yamada Y, Ohe Y, Yoshida T, Minami H, Ohtsu A, Matsumura Y, Saijo N, Okuda H (2010) Association of carboxylesterase 1A genotypes with irinotecan pharmacokinetics in Japanese cancer patients. Br J Clin Pharmacol 70 (2):222–233. doi:10.1111/j.1365-2125.2010.03695.x
14. Heinig K, Bucheli F (2008) Sensitive determination of oseltamivir and oseltamivir carboxylate in plasma, urine, cerebrospinal fluid and brain by liquid chromatography-tandem mass spectrometry. J Chromatogr B Analyt Technol Biomed Life Sci 876(1):129–136. doi:10.1016/j.jchromb.2008.10.037
15. Holmes RS, Wright MW, Laulederkind SJ, Cox LA, Hosokawa M, Imai T, Ishibashi S, Lehner R, Miyazaki M, Perkins EJ, Potter PM, Redinbo MR, Robert J, Satoh T, Yamashita T, Yan B, Yokoi T, Zechner R, Maltais LJ (2010) Recommended nomenclature for five mammalian carboxylesterase gene families: human, mouse, and rat genes and proteins. Mamm Genome 21(9–10):427–441. doi:10.1007/s00335-010-9284-4
16. Geshi E, Kimura T, Yoshimura M, Suzuki H, Koba S, Sakai T, Saito T, Koga A, Muramatsu M, Katagiri T (2005) A single nucleotide polymorphism in the carboxylesterase gene is associated with the responsiveness to imidapril medication and the promoter activity. Hypertens Res 28(9):719–725. doi:10.1291/hypres.28.719
17. He G, Massarella J, Ward P (1999) Clinical pharmacokinetics of the prodrug oseltamivir and its active metabolite Ro 64-0802. Clin Pharmacokinet 37(6):471–484
18. Ogihara T, Kano T, Wagatsuma T, Wada S, Yabuuchi H, Enomoto S, Morimoto K, Shirasaka Y, Kobayashi S, Tamai I (2009) Oseltamivir (tamiflu) is a substrate of peptide transporter 1. Drug Metab Dispos 37(8):1676–1681. doi:10.1124/dmd.109.026922
19. Snell P, Dave N, Wilson K, Rowell L, Weil A, Galitz L, Robson R (2005) Lack of effect of moderate hepatic impairment on the pharmacokinetics of oral oseltamivir and its metabolite oseltamivir carboxylate. Br J Clin Pharmacol 59(5):598–601. doi:10.1111/j.1365-2125.2005.02340.x
20. Schwarz R, Kaspar A, Seelig J, Kunnecke B (2002) Gastrointestinal transit times in mice and humans measured with 27Al and 19 F nuclear magnetic resonance. Magn Reson Med 48(2):255–261. doi:10.1002/mrm.10207
21. Morimoto K, Kishimura K, Nagami T, Kodama N, Ogama Y, Yokoyama M, Toda S, Chiyoda T, Shimada R, Inano A, Kano T, Tamai I, Ogihara T (2011) Effect of milk on the pharmacokinetics of oseltamivir in healthy volunteers. J Pharm Sci 100(9):3854–3861. doi:10.1002/jps.22627
22. Anderle P, Nielsen CU, Pinsonneault J, Krog PL, Brodin B, Sadee W (2006) Genetic variants of the human dipeptide transporter PEPT1. J Pharmacol Exp Ther 316(2):636–646. doi:10.1124/jpet.105.094615
23. Morimoto K, Nakakariya M, Shirasaka Y, Kakinuma C, Fujita T, Tamai I, Ogihara T (2008) Oseltamivir (Tamiflu) efflux transport at the blood-brain barrier via P-glycoprotein. Drug Metab Dispos 36 (1):6–9. doi:10.1124/dmd.107.017699
24. Ose A, Ito M, Kusuhara H, Yamatsugu K, Kanai M, Shibasaki M, Hosokawa M, Schuetz JD, Sugiyama Y (2009) Limited brain distribution of [3R,4R,5 S]-4-acetamido-5-amino-3-(1-ethylpropoxy)-1-cyclohexene-1-carboxyl ate phosphate (Ro 64-0802), a pharmacologically active form of oseltamivir, by active efflux across the blood-brain barrier mediated by organic anion transporter 3 (Oat3/Slc22a8) and multidrug resistance-associated protein 4 (Mrp4/Abcc4). Drug Metab Dispos 37(2):315–321. doi:10.1124/dmd.108.024018
25. Hoffmeyer S, Burk O, von Richter O, Arnold HP, Brockmoller J, Johne A, Cascorbi I, Gerloff T, Roots I, Eichelbaum M, Brinkmann U (2000) Functional polymorphisms of the human multidrug-resistance gene: multiple sequence variations and correlation of one allele with P-glycoprotein expression and activity in vivo. Proc Natl Acad Sci USA 97(7):3473–3478. doi:10.1073/pnas.050585397
26. Abla N, Chinn LW, Nakamura T, Liu L, Huang CC, Johns SJ, Kawamoto M, Stryke D, Taylor TR, Ferrin TE, Giacomini KM, Kroetz DL (2008) The human multidrug resistance protein 4 (MRP4, ABCC4): functional analysis of a highly polymorphic gene. J Pharmacol Exp Ther 325(3):859–868. doi:10.1124/jpet.108.136523

Drug Metab. Pharmacokinet. 28 (3): 250–259 (2013).

Regular Article

Hepatocyte Nuclear Factor 6 Activates the Transcription of *CYP3A4* in Hepatocyte-like Cells Differentiated from Human Induced Pluripotent Stem Cells

Takamitsu SASAKI[1], Shogo TAKAHASHI[1], Yoshihiro NUMATA[1], Masayo NARITA[1], Yutaka TANAKA[1], Takeshi KUMAGAI[1], Yuki KONDO[2], Tamihide MATSUNAGA[2], Shigeru OHMORI[3,4] and Kiyoshi NAGATA[1,*]

[1]*Department of Environmental and Health Science, Tohoku Pharmaceutical University, Sendai, Japan*
[2]*Department of Clinical Pharmacy, Graduate School of Pharmaceutical Sciences, Nagoya City University, Nagoya, Japan*
[3]*Department of Molecular Pharmacology, Shinshu University Graduate School of Medicine, Matsumoto, Japan*
[4]*Department of Pharmacy, Shinshu University Hospital, Matsumoto, Japan*

Full text of this paper is available at http://www.jstage.jst.go.jp/browse/dmpk

Summary: Human induced pluripotent stem cells (iPSCs) are a valuable source of hepatocytes for applications in drug metabolism studies. However, the current protocols for generating iPSC-derived hepatocyte-like cells (iPSHCs) are still very inefficient, and iPSHCs do not have sufficient hepatocyte-specific features, which include expression of a series of hepatocyte-specific genes, such as those encoding cytochrome P450 (*CYP*). In this study, we investigated whether introduction of human hepatocyte nuclear factor 6 (HNF6) could modulate the expression of *CYP3A4* and other *CYP* genes in iPSHCs as well as in HepG2 cells, a fetal liver cell line (HFL cells), and in hepatocytes. *CYP3A4* mRNA could be detected in iPSHCs, but the expression level was very low compared with those in HepG2 cells and hepatocytes. However, the *CYP3A4* mRNA levels markedly increased on introduction of HNF6 and reached one-tenth of those in hepatocytes. We also found that HNF6 introduction increased *CYP3A4* gene transcription in HFL cells and HepG2 cells, which have features similar to those of fetal hepatocyte-like cells; however, it did not affect *CYP3A4* mRNA expression in hepatocytes. These results suggest that HNF6 plays an important role in the gene regulation of *CYP3A4* during development from the fetal period to the postnatal period.

Keywords: CYP3A4; differentiation; hepatocytes; HNF6; induced pluripotent stem cells; liver-enriched transcription factors

Introduction

Human primary hepatocytes and HepG2 cells are often used to study transcriptional activation of genes implicated in cytochrome P450 (*CYP*) expression.[1)] Human hepatocytes that retain liver-specific functions have an entire repertoire of hepatic drug-metabolizing enzymes. However, these cells show a large donor-to-donor variability in drug metabolizing activity and induction response, resulting in difficulties in interpreting data from different sources.[2)] Cell lines, such as HepG2 cells, are available and can easily be standardized among laboratories, but have low expression levels of *CYP* genes and liver-enriched transcription factors (LETFs).[3,4)]

Recently, human induced pluripotent stem cells (iPSCs) were established from fibroblast cells by introducing Oct3/4, Sox2, Klf4, and c-Myc; these cells can differentiate into most body cell types and may serve as an ideal renewable source of functional human hepatocytes.[5)] Several studies have demonstrated the capacity of iPSCs to differentiate into hepatocyte-like cells under chemically defined conditions.[6–8)] However, the current protocols for generating iPSC-derived hepatocyte-like cells (iPSHCs) are inefficient, and these cells do not possess a range of hepatocyte-specific fea-

Received November 17, 2012; Accepted December 7, 2012
J-STAGE Advance Published Date: January 1, 2013, doi:10.2133/dmpk.DMPK-12-RG-132
**To whom correspondence should be addressed:* Kiyoshi NAGATA, *Department of Environmental and Health Science, Tohoku Pharmaceutical University, 4-4-1, Komatsushima, Aoba-ku, Sendai 981-8558, Japan. Tel. +81-22-727-0133, Fax. +81-275-2013, E-mail: nagataki@tohoku-pharm.ac.jp*
This work was supported by a Health and Labour Sciences Research Grant for Research on Food Safety (No. 22230301) from the Ministry of Health, Labour and Welfare of Japan; by a Grant-in-Aid for Scientific Research (B) (No. 23790193); and by the Japanese Ministry of Education, Culture, Sports, Science and Technology (MEXT)-Supported Program for the Strategic Research Foundation at Private Universities.

tures, including expression of *CYP*. Thus, the current protocols still require the use of multiple growth factors, cytokines, and low molecular weight compounds, as well as the introduction of hepatic lineage stage-specific genes, such as those encoding LETFs, to modify these cells appropriately.

The expression of many hepatocyte-specific genes in the adult liver is regulated by LETFs, including hepatocyte nuclear factor 1 (HNF1), HNF3, HNF4, HNF6, and CCAAT/enhancer binding protein (c/EBP); these are all key components in the differentiation process in the adult liver.[9] Many studies have identified HNF4α as a direct transactivator of *CYP* genes.[10,11] Kamiyama *et al.* reported that knocking down HNF4α affects the expression of the major drug metabolizing CYPs.[12] Other LETFs, HNF1α, HNF3, and c/EBP, also play an important role in the regulation of many *CYP*s.[13–18] In addition to directly acting as transcriptional regulators of *CYP* genes, these LETFs control each other's expression and the expression of *CYP* genes through a network of cooperative and synergistic effects.

HNF6, a member of the Onecut family of transcription factors, controls the expression of other LETFs.[19–23] It is expressed in the liver, pancreas, and nervous system during embryonic development.[24] In the liver, HNF6 is detected in hepatoblasts and then later in the cholangiocytes and hepatocytes, where it is continually expressed in adults.[24–27] Fetuses of *HNF6*-knockout mice exhibit delayed expression of glucose-6-phosphatase, which catalyzes the final step of gluconeogenesis and is a late marker of hepatocyte maturation.[28] HNF6 also regulates *in vivo* hepatic expression of cholesterol 7α-hydroxylase (CYP7A1), which is only marginally expressed in fetal livers, but is strongly expressed in the liver postnatally.[29] Thus, HNF6 may play an important role in regulation of hepatocyte-specific genes during liver maturation.

As with CYP7A1, CYP3A4 expression significantly changes during ontogeny; CYP3A4 is the most abundant of CYP enzymes in adult human livers.[30,31] Thus, the expression level of CYP3A4 is highly correlated with LETF-mediated hepatocyte differentiation. Therefore, the mechanism regulating *CYP3A4* expression needs to be elucidated to understand the process of generating mature hepatocyte-like cells differentiated from iPSCs. Moreover, the precise role of HNF6 in the regulation of *CYP3A4* and other drug-metabolizing *CYP* genes during liver maturation remains unclear.

In this study, we aimed to determine whether HNF6 could modulate the expression of *CYP3A4* and other *CYP* genes in iPSHCs, by comparing gene expression in immature hepatocytes (HepG2 cells and fetal liver cell line [HFL] cells) and hepatocytes after HNF6 introduction. Our results indicated that HNF6 is strongly involved in *CYP3A4* expression in iPSHCs and immature hepatocytes, suggesting that HNF6 plays an important role in *CYP3A4* regulation during the maturation of liver cells from the fetal to the postnatal stage.

Materials and Methods

Materials: *Bgl*II and *Sal*I were purchased from Nippon Gene Co., Ltd. (Tokyo, Japan). Dexamethasone (DEX), 2-mercaptoethanol (2-ME), oncostatin M (OSM), and Y-27632 were purchased from Wako Pure Chemicals (Osaka, Japan). Mitomycin C and sodium butyrate were purchased from Sigma (St. Louis, MO). Activin, basic fibroblast growth factor (bFGF), and hepatocyte growth factor (HGF) were purchased from Peprotech (Rocky Hill, NJ). Testosterone was purchased from Tokyo Chemical Industry Co., Ltd. (Tokyo, Japan). 6β-Hydroxytestosterone was purchased from BD Biosciences (Heidelberg, Germany). Dimethyl sulfoxide (DMSO) was obtained from Nacalai Tesque (Kyoto, Japan), and other reagents used in the study were commercial products of analytical grade. Oligonucleotides were commercially synthesized by Fasmac (Atsugi, Japan).

Construction of recombinant adenovirus: The open reading frame of *HNF6* was PCR amplified from cDNA obtained from HepG2 cells using the forward primer 5′-ccgagatctCGATGAACGCGCAGCTGACC-3′ and the reverse primer 5′-ccggtcgacTTCATGCTTTGGTACAAGTGC-3′, in which lower case letters represent *Bgl*II and *Sal*I restriction sites, respectively. The amplified fragments were subcloned into the pCR4-TOPO vector (Invitrogen Co., Carlsbad, CA). The plasmid was then digested with *Bgl*II and *Sal*I and was ligated into the corresponding sites of pShuttle-CMV (MP Biomedicals, Solon, OH). Human HNF6-expressing adenovirus (AdhHNF6) was prepared using the AdEasy™ System (Quantum Biotechnologies, Montreal, Canada) as reported previously.[32] Control adenovirus, *i.e.*, a β-galactosidase-expressing adenovirus (AdLacZ), was provided by Dr. Izumi Saito (The University of Tokyo, Tokyo, Japan). The titer of recombinant adenoviruses, 50% tissue culture infectious dose (TCID50), was determined as reported previously.[32] Multiplicity of infection (MOI) was calculated by dividing the TCID50 by the number of cells.

Cell line and cell culture: HepG2 cells were purchased from the RIKEN cell bank (Tsukuba, Japan). Cells were cultured in Dulbecco's modified Eagle's medium (DMEM; Wako Pure Chemicals) supplemented with 10% fetal bovine serum (FBS; Biowest, Miami, FL), minimum essential medium nonessential amino acids (MEM NEAA; Invitrogen), and Antibiotic-Antimycotic (Invitrogen), under 5% CO_2 at 37°C. The cells were seeded in 24-well tissue culture plates (BD Biosciences) at 1.0×10^5 cells per well at 1 d before adenovirus infection. After 72 h, these cells were harvested and total RNA was extracted. Whole cell lysates and total RNA were used for immunoblot analysis and real-time PCR, respectively.

Human primary hepatocyte cells and cell culture: Human fetal hepatocytes were obtained from Applied Cell Biology Research Institute (Kirkland, WA) and cultured in Williams' medium E (Sigma) containing 10% FBS (Biowest), 2 mM L-glutamine (Invitrogen), and antibiotics (Sigma) under 5% CO_2 at 37°C.[33] Human cryopreserved primary hepatocytes (lot HEP187170, 26-year-old Caucasian woman) were purchased from Biopredic International (Rennes, France). The hepatocytes were thawed and cultured using the medium kit according to the manufacturer's protocol. Fetal and adult hepatocytes were seeded in type I collagen-coated 24-well tissue culture plates (Sumitomo Bakelite Co. Ltd., Tokyo, Japan) at 5.0×10^4 and 1.0×10^5 cells per well, respectively, at 1 d before adenovirus infection. After 72 h, total RNA was extracted and used for real-time PCR.

Dual-reporter assays: The luciferase reporter plasmids, pGL3-basic and pGL4.82, were purchased from Promega (Madison, WI). Construction of the *CYP3A4* luciferase reporter plasmid, pCYP3A4-362-7.7k, has been described previously.[34]

HepG2 cells were plated into 48-well tissue culture plates (BD Biosciences) at a density of 6.0×10^4 cells and were then transfected with pCYP3A4-362-7.7k (0.4 μg) and pGL4.82 (0.1 μg), as an internal control, using Targefect F-1 (Nacalai Tesque). The next day, the cell medium was exchanged for culture medium and the cells were infected with the respective recombinant adenoviruses.

Table 1. Primers used for real-time PCR

Genes	Forward primers (5′–3′)	Reverse primers (5′–3′)	Reference
CYP1A1	CATCCCCCACACACAACA	CAGGGGTGAGAAACCGTTCA	35)
CYP1A2	AGTCCAGGAGCAGTATCAGG	CCTGCTCCAAAGATGTCATT	—
CYP2C9	CCTCTGGGGCATTATCCATC	ATATTTGCACAGTGAAACATAGGA	36)
CYP2C19	TTCATGCCTTTCTCAGCAGG	ACAGATAGTGAAATTTGGACC	36)
CYP2D6	GCCTTCCTGCCTTTCTCAGCAG	ATGGGTCACCAGGAAAGCAAA	37)
CYP3A4	CTGTGTGTTTCCAAGAGAAGTTAC	TGCATCAATTTCCTCCTGCAG	38)
CYP3A7	AGATTTAATCCATTAGATCCATTCG	AGGCGACCTTCTTTTATCTG	38)
CYP7A1	CAGAACTGAATGACCTGCCA	GGTGCAAAGTGAAATCCTCC	39)
AFP	AGCTTGGTGGTGGATGAAAC	CCCTCTTCAGCAAAGCAGAC	40)
ALB	TGGCACAATGAAGTGGGTAA	CTGAGCAAAGGCAATCAACA	41)
HNF6	GAAGGATAGAGGCAACACA	AGTTGCTGACAGTGCTCAG	—
GAPDH	CATGGGTGTGAACCATGAGAA	GGTCATGAGTCCTTCCACGAT	42)

After 72 h, cells were suspended in 0.1 mL passive lysis buffer (Promega). Reporter activities were determined using the Dual-Luciferase® Reporter Assay system (Promega). Luminescence derived from reactions using the reporter assay was monitored using a Glomax™ 96 Microplate Luminometer (Promega).

Human induced pluripotent stem cell culture: Human iPSCs, #51 Windy, were provided by Dr. Akihiro Umezawa, National Research Institute for Child Health and Development. The iPSCs were maintained in DMEM/F12 (Sigma) with 20% knockout serum replacement (KSR, Invitrogen), 2 mM L-glutamine (Invitrogen), 0.08 mM MEM NEAA (Invitrogen), 0.1 mM 2-ME, and 5 ng/mL bFGF, on mitomycin C-treated mouse embryonic fibroblasts (Oriental Yeast Co., Ltd., Tokyo, Japan). Cells were cultured under 5% CO_2 at 37°C.

Differentiation of human iPSCs: For induction of definitive endoderm, iPSCs were cultured for 3 d with Roswell Park Memorial Institute 1640 medium (RPMI 1640, Invitrogen) supplemented with 0.5% FBS, GlutaMAX (Invitrogen), 1 mM sodium butyrate, antibiotics (Sigma), and 100 ng/mL activin. Medium was refreshed on the second day. Subsequently, the differentiated cells were incubated in RPMI 1640 containing 2% KSR, GlutaMAX, 0.5 mM sodium butyrate, antibiotics (Sigma), and 100 ng/mL activin for 2 d.

For induction of hepatoblasts, the iPSC-derived definitive endoderms were treated with 10 nM Y-27632 for 1 h and were then passaged with Accutase (Innovative Cell Technologies, Inc., San Diego, CA). Cells were plated onto Matrigel™-coated (BD Matrigel™ Basement Membrane Matrix Growth Factor-Reduced, BD Biosciences) 24-well tissue culture plates (Sumitomo Bakelite Co., Ltd.) in KnockOut™ DMEM (Invitrogen), which was supplemented with 20% KSR, GlutaMAX, 0.1 mM NEAA, 0.1 mM 2-ME, antibiotics, and 1% DMSO. Medium was replaced every other day, and hepatoblast differentiation was continued for a further 7 d.

The iPSC-derived hepatoblasts were induced to differentiate into hepatocytes by switching to modified Lanford medium (Primary Cell Co., Ltd., Sapporo, Japan) supplemented with 10 ng/mL HGF, 20 ng/mL OSM, and 100 nM DEX. Cells were cultured for 14 d, and hepatic differentiation medium was refreshed every 2–3 d. In this hepatic maturation period, the cells were cultured and infected with AdhHNF6 (100 MOI) using 4 conditions (described below). Cells were then incubated with 0.2 mL of the recombinant adenovirus-containing medium for 1 h, followed by the addition of 0.8 mL medium.

For condition 1, the cells were infected with AdhHNF6 on day 15. After 3 d, the cells were recovered; thus, under condition 1, the culture period was 18 d. Under condition 2, the cells were infected with AdhHNF6 on day 19. After 3 d, the cells were recovered, totaling a culture period of 22 d. Under condition 3, the cells were infected with AdhHNF6 on day 22. After 3 d, the cells were recovered, resulting in a culture period of 25 d. Under condition 4, the cells were infected with AdhHNF6 on both days 19 and 22. Six days after the first infection, the cells were recovered, resulting in a culture period of 25 d. After these cells were harvested, total RNA extracted and whole cell lysates prepared were used to carry out real-time PCR and immunoblot analyses, respectively.

RNA purification and real-time PCR: Total RNA was extracted using TRI Reagent® (Molecular Research Center, Cincinnati, OH). First-strand cDNA was synthesized from 2 μg total RNA in a 25-μL reaction mixture using Moloney Murine Virus Reverse Transcriptase (Promega), oligo$(dT)_{20}$ primer, and a ribonuclease inhibitor (TaKaRa Bio, Kyoto, Japan). The cDNA was used for real-time PCR with SYBR Premix ExTaq (TaKaRa Bio) to measure mRNA levels of liver-specific genes, *CYPs*, and *glyceraldehyde-3-phosphate dehydrogenase* (*GAPDH*). Amplification reactions were performed with specific primers (**Table 1**).[35–42] Quantitative values were obtained above the threshold PCR cycle number (Ct) at which the increase in signal associated with an exponential growth in PCR products was detected using Thermal Cycler Dice™ TP800 (TaKaRa Bio). Relative mRNA expression levels in each sample were normalized to *GAPDH* expression levels.

Immunoblot analysis: Immunoblot analysis was performed to detect the expression of HNF6 proteins in HepG2 cells and iPSC-derived hepatocyte-like cells (iPSHCs). Whole cell lysate from these cells that had been infected with AdhHNF6 were size-fractionated by gel electrophoresis on a 10% polyacrylamide/0.1% sodium dodecyl sulfate gel, after being denatured by heating in a 2-ME-containing loading buffer. The proteins were electrotransferred to Immobilon®-P membranes (Millipore, Billerica, MA), which were then incubated for 1 h with polyclonal goat anti-human HNF6 antibody (Santa Cruz Biotechnology, Inc., Santa Cruz, CA) that had been diluted in Tris-buffered saline (1:1,000). The membranes were subsequently incubated for 1 h with a horseradish peroxidase-conjugated secondary antibody diluted in Tris-buffered saline (1:10,000; Santa Cruz Biotechnology, Inc.). After development with SuperSignal West Pico chemiluminescent substrate (Thermo Fisher Scientific Inc., Waltham, MA), the membrane was scanned using a Lumino Imaging Analyzer FAS-1000 (Toyobo, Osaka, Japan).

Determination of testosterone 6β-hydroxylase activity: Testosterone 6β-hydroxylase activity was determined as described previously with minor modification.[43] All iPSCs, iPSHCs,